JOURNAL OF GUIDANCE, CONTROL, AND DYNAMICS
Vol. 28, No. 5, September–October 2005

Robust Integrated Flight Control Design Under Failures, Damage, and State-Dependent Disturbances

Jovan D. Bošković,* Sarah E. Bergstrom,† and Raman K. Mehra‡
Scientific Systems Company, Inc., Woburn, Massachusetts 01801

A robust integrated fault-tolerant flight control system is presented that accommodates different types of actuator failures and control effector damage, even while rejecting state-dependent disturbances. It is shown that a decentralized failure detection, identification, and reconfiguration system, combined judiciously with adaptive laws for damage estimates and variable structure adjustment laws for disturbance estimates, yields a stable system despite simultaneous presence of failures, damage and disturbances. The proposed system is well suited for the case of first-order actuator dynamics. The properties of the proposed algorithms are illustrated on a medium-fidelity nonlinear simulation of Boeing's Tailless Advanced Fighter Aircraft.

I. Introduction

TO increase the autonomy of unmanned aerial vehicles (UAV) and the duration of their autonomously performed missions, the flight control systems (FCS) for UAVs need to be capable of accommodating a large class of subsystem and component failures and structural damage without substantially affecting the performance of the overall system. In this context, important components of the FCS are on-line failure detection, identification, and reconfiguration (FDIR) algorithms the role of which is to rapidly and accurately detect and identify different failures and faults and appropriately reconfigure the control laws to maintain the stability of the system.

To be able to accommodate different faults and failures, the FDIR system commonly needs to effectively integrate several FDIR algorithms. For instance, sensor failure algorithms need to be integrated with actuator failure accommodation subsystem, and the resulting system needs to be integrated with the algorithms capable of accommodating structural damage and resulting disturbances. One of the major issues in the FDIR design is the complexity of the resulting algorithms and their interactions that, if not taken into account, can lead to substantial performance deterioration and even instability in the system. The main challenge in this context is to arrive at a FDIR system that is capable of accommodating such faults and failures even while minimizing the interactions between the FDIR subsystems. In this paper a design of an integrated algorithm that achieves the FDIR objective and maintains the desired performance of the system is described.

The focus of the study presented here is on flight-critical failures and faults. In particular, the analysis and design are concentrated on actuator failures and control effector damage that generates large state-dependent disturbances. Both types of faults, if not rapidly accommodated, can lead to substantial performance degradation and instability of the closed-loop system. The design challenge in this context is an integration of the actuator failure and control effector damage FDIR subsystems with disturbance rejection algorithms, which results in a stable overall system.

Most of the available FDIR techniques for flight-critical faults and failures address either actuator failures or control effector damage. An integration of the resulting FDIR subsystems and minimization of their interactions has not been studied. In addition, some of the available FDIR algorithms are well suited for linear models, whereas those suitable for nonlinear aircraft dynamics are based on-neural networks where a large number of parameters needs to be adjusted. In addition, these algorithms are based on direct adaptive control and, hence, do not provide FDIR information that is useful for condition-based maintenance. An overview of the existing results is given next.

Several results involving FDIR based on linearized models of aircraft dynamics have been reported.[1–10] An application of multivariable adaptive control techniques to flight control reconfiguration was considered.[1] The objective was to redesign automatically flight control laws to compensate for actuator failures or surface damage. A reconfigurable control scheme based on on-line parameter estimation and linear quadratic control algorithms was evaluated on a nonlinear simulation of the F-16 aircraft.[2] A scheme combining constrained least-squares identification of uncertain stability and control derivatives and a receding horizon optimal control law was developed and flight tested on a VISTA/F-16 aircraft.[3] A similar approach based on static constrained identification and prior information was used[4] to estimate time-varying parameters arising as a result of failures and was evaluated on a F-16 aircraft simulation. A common feature of these schemes is that they were developed for linearized models of aircraft dynamics and are well suited for single actuator failures. The techniques are based on on-line estimation of a large number of uncertain parameters associated with failures, which can result in slow response and large transients.

A neural-network-based adaptive control approach[5] was developed and evaluated on a simulation of F/A-18 aircraft. A similar approach was applied to the Boeing's Tailless Advanced Fighter Aircraft (TAFA).[6] The neural network was used to compensate for the plant inversion error as a result of modeling uncertainties, failures, and damage. This algorithm was combined with on-line control allocation based on identification of control derivatives. The properties of the overall control system were evaluated on a high-fidelity TAFA simulation.[6] These algorithms were successfully evaluated through hardware-in-the-loop simulations and flight testing on a X-36 tailless fighter aircraft.[7] Although these algorithms have the potential to deal simultaneously with actuator failures and nonlinearities arising as a result of control effector damage, their utility in that context has yet to be demonstrated. In addition, neural networks require on-line adjustment of a large number of parameters (weights), which can require very complex tuning in different flight regimes.

It is of interest to extend the existing results in the area of FDIR to the case of simultaneous actuator failures and control effector

Presented as Paper 2003-5490 at the AIAA Guidance, Navigation, and Control Conference, Austin, TX, 11–14 August 2003; received 3 June 2004; revision received 19 October 2004; accepted for publication 7 December 2004.

*Autonomous and Intelligent Control Systems Group Leader, 500 W. Cummings Park, Suite 3000; jovan@ssci.com. Senior Member AIAA.

†Research Engineer, 500 W. Cummings Park, Suite 3000; jovan@ssci.com.

‡President and CEO, 500 W. Cummings Park, Suite 3000; rkm@ssci.com. Member AIAA.

damage accommodation, arrive at a design that adjusts a moderate number of adaptive parameters, minimizes the interactions between the resulting FDIR subsystems, and effectively compensates for the nonlinearities arising as a result of the damage. Some of the results that address some of the aspects of this problem are described next.

The approach from Ref. 8 addresses the problem of a large number of adjustable parameters encountered in the existing FDIR designs by parameterizing a large class of actuator failures using only two parameters, and, based on on-line estimation of these parameters and their use in the reconfigurable control law, ensures fast failure FDI and robust control reconfiguration. In another paper,[9] control effector damage problem was addressed using both gradient adaptation and a variable structure algorithm. In both cases the stability of the overall system is ensured despite damage of multiple control effectors. However, it was also assumed that there are no damage-generated nonlinearities.

To address the issues arising in the context of integrated FDIR, in this paper a robust integrated fault-tolerant flight control design that effectively compensates for actuator failures, control effector damage, and large damage-generated state-dependent disturbances is proposed. Advantages of the proposed technique are as follows:

1) It solves the FDIR problem for simultaneous actuator failure and control effector damage even while rejecting resulting large state-dependent disturbances and minimizing interactions between the FDIR subsystems.

2) It uses a moderate number of adjustable parameters ($3m+6$, where m is the number of control effectors). This number can be further decreased if the FDI for actuator and control effectors that are less used in a particular flight regime is turned off.

3) It is well suited for nonlinear aircraft dynamics. As shown in the paper, the proposed approach is well suited for nonlinear models that are affine in the control input and are characterized by sufficiently smooth nonlinearities.

4) It extends previous results by the authors,[8] developed for linearized models of aircraft dynamics and actuator FDIR only, to nonlinear aircraft dynamics and simultaneous actuator failure and control effector damage accommodation.

The proposed approach is based on the decentralized FDIR scheme for actuator failure accommodation[8] and is extended here to include control effector damage and nonlinear aircraft dynamics and state-dependent disturbances. The main idea behind the proposed approach is described next. The overall FDIR system includes decentralized FDI systems for each of the actuators and a damage and disturbance estimation module that estimates the extent of the control effector damage and resulting state-dependent disturbances. The system also includes a robust reconfigurable controller that uses the estimates of failure- and damage-related parameters and disturbances to ensure robust tracking and is shown in Fig. 1. In the case of failure or damage, the FDIR system will accurately detect the failed actuator or control effector if there is enough persistent excitation in the system. However,even in the case of poor excitation of the signals, the overall system will be stabilized despite the simultaneous effect of failures, damage, and disturbances. In such a case additional tests can be run to accurately identify the failure. The design of the system from Fig. 1 is described in detail in this paper.

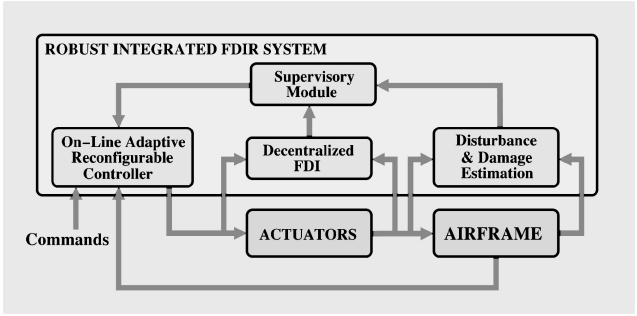

Fig. 1 Proposed robust supervisory FDIR system (©1999–2004 Scientific Systems Company, Inc.).

II. Problem Statement

In this paper the focus is on the class of models of aircraft dynamics of the form

$$\dot{z}_1 = \bar{f}(z) \tag{1}$$

$$\dot{z}_2 = f_0(z) + G_0(z)u + \xi_0(z) \tag{2}$$

$$\dot{u} = -\lambda(u - u_c) \tag{3}$$

where $z : \mathbb{R}^+ \to \mathbb{R}^n$ denotes the state vector; $z_1 : \mathbb{R}^+ \to \mathbb{R}^{(n-p)}$, $z_2 : \mathbb{R}^+ \to \mathbb{R}^p$, $z = [z_1^T \;\; z_2^T]^T$, $\bar{f} : \mathbb{R}^n \to \mathbb{R}^{(n-p)}$, $f_0 : \mathbb{R}^n \to \mathbb{R}^p$, $G_0 : \mathbb{R}^n \to \mathbb{R}^{p\times m}$, $u_c : \mathbb{R}^+ \to \mathbb{R}^m$, and $u : \mathbb{R}^+ \to \mathbb{R}^m$ denote respectively the controller output vector and the plant input vector; $\xi_0 : \mathbb{R}^n \to \mathbb{R}^p$ denotes an uncertain disturbance vector; and $\lambda \gg 1$ denotes the actuator gain. It is assumed that the preceding model describes the dominant dynamics of the aircraft. In such a case, the state variables include total velocity V; angle of attack α; sideslip angle β; angular velocities p, q, and r; and attitude angles ϕ, θ, and ψ. In addition, it is assumed that the nonlinearities $f_0(z)$ and $G_0(z)$ are associated with nominal aircraft dynamics [i.e., the dynamics in flight regimes in which there are no failures or damage and where $\xi_0(z) = 0$], and $\xi_0(z)$ is an unknown nonlinearity generated by failures or damage.

The preceding model is subject to the following assumption.

Assumption 1:

a) State of the system is measurable.

b) For a closed bounded set of states $\mathcal{S}_z$, $G_0(z)G_0^T(z)$ is invertible for all $z \in \mathcal{S}_z$.

c) $f_0(z)$, $G_0(z)$, and $\xi_0(z)$ are sufficiently smooth functions (functionals) of their argument.

d) $m > p$.

e) At least p actuators are highly reliable and can be assumed to be fault tolerant over an interval of interest.

f) $|\xi_{0i}| \le c_{0i} + d_{0i}\varphi_{0i}(z)$, where $\varphi_0(z) = [\varphi_{01}(z) \;\; \varphi_{02}(z) \ldots \varphi_{0p}(z)]^T$ is a known vector function of the state, $\varphi_0(0) = 0$, and $c_{0i} \ge 0$ and $d_{0i} \ge 0$ are known.

Because the nonlinear model (1) and (2) describes the dynamics of the dominant state variables, these are commonly measurable in the case of advanced fighter aircraft. Hence, assumption 1a is justified in most practical situations. In the case of gain-scheduled models of aircraft dynamics, the aerodynamics effects are modeled as $A(z)$ and $B(z)$, where the matrices A and B depend on several variables including the Mach number, altitude, angle of attack, and sideslip angle. Each element of A and B can then be obtained from the look-up tables and represented as a multidimensional polynomial of these state variables. In most of the flight regimes, the resulting matrix $B(z)$ is such that $B(z)B^T(z)$ is invertible over a domain. Assumption 1b is justified in such cases. Although assumption 1c is commonly justified in the case of nominal nonlinear aircraft dynamics (i.e., the case when $\xi_0 = 0$), it might not be satisfied in the case of the nonlinearity $\xi_0(z)$ generated by failures or damage. However, as a first approximation, smoothness of $\xi_0(z)$ is assumed to keep the problem analytically tractable. Assumption 1d is justified in the case of advanced fighter aircraft characterized by a high level of control effector redundancy. Because of assumption 1e, up to $m - p$ multiple simultaneous failures are allowed to occur. This is not a restrictive assumption for modern combat aircraft because, for instance, in the case of Boeing's TAFA, $m - p = 6$. It is also noted that some previous information regarding the nonlinearity $\xi_0(z)$ is assumed. This is justified in the case when the effect of failures and damage on the aerodynamics is explicitly modeled based on wind-tunnel data, similarly as in the case of wing damage.[11]

The model (1) and (2) is not in a convenient form because model-reference control design results in a nonlinear reference model that also depends on the state of the system.[12] On the other hand, it turns out that the models of aircraft dynamics have some convenient properties that can be used to transform them to a controllable canonical form. For this reason the following assumption is considered:

Assumption 2: Vector $\bar{f}(z)$ can be expressed in the form $\bar{f}(z) = F(z_1)z_2$, where $F(z_1)$ is smooth and invertible on a closed bounded domain $\mathcal{S}_z$.

This assumption is justified in the case when $z_1 = [\phi \ \ \theta \ \ \psi]^T$, and a subvector $\bar{z}_2$ of vector z_2 is the vector of angular velocities in the body frame $\bar{z}_2 = [p \ \ q \ \ r]^T$. In such a case one has

$$\begin{bmatrix} \dot{\phi} \\ \dot{\theta} \\ \dot{\psi} \end{bmatrix} = \begin{bmatrix} 1 & \sin\phi\tan\theta & \cos\phi\tan\theta \\ 0 & \cos\phi & -\sin\phi \\ 0 & \sin\phi\sec\theta & \cos\phi\sec\theta \end{bmatrix} \begin{bmatrix} p \\ q \\ r \end{bmatrix} \tag{4}$$

$$= R(\phi, \theta)\omega \tag{5}$$

where $\omega = [p \ \ q \ \ r]^T$. It can be readily shown that $R(\phi, \theta)$ is invertible for all $\theta \in (-\pi/2, \pi/2)$.

Coordinate transformation: Under assumption 2, $F(z_1)$ is now chosen as the transformation matrix for the z_1 subsystem, and a time derivative of Eq. (1) is taken to obtain

$$\begin{aligned} \ddot{z}_1 &= \dot{F}(z_1)z_2 + F(z_1)\dot{z}_2 \\ &= \left[\frac{\partial F}{\partial z_1}F(z_1)z_2\right]z_2 + F(z_1)[f_0(z) + G_0(z)u + \xi_0(z)] \\ &= f_1(z_1, z_2) + G_1(z_1, z_2)u + \xi_1(z_1, z_2) \end{aligned} \tag{6}$$

where $f_1(z_1, z_2) = [(\partial F/\partial z_1)F(z_1)z_2]z_2 + F(z_1)f_0(z)$, $G_1(z_1, z_2) = F(z_1)G_0(z)$, and $\xi_1(z_1, z_2) = F(z_1)\xi_0(z)$. The matrix $G_1(z)\,G_1(z)^T$ is invertible on the domain $\mathcal{S}_z$ because, under assumptions 1b and 2, both $G_0(z)G_0^T(z)$ and $F(z_1)$ are invertible on the same domain.

The following change of variables in now introduced: $x_1 = z_1$, and $x_2 = \dot{z}_1$. The relationship between z_2 and x_2 is obtained from the inverse transformation: $z_2 = F^{-1}(z_1)\dot{z}_1 = F^{-1}(x_1)x_2$. Hence,

$$\dot{x}_1 = x_2 \tag{7}$$

$$\dot{x}_2 = f_1\left(x_1, F^{-1}(x_1)x_2\right) + G_1\left(x_1, F^{-1}(x_1)x_2\right)u + \xi_1\left(x_1, F^{-1}(x_1)x_2\right) \tag{8}$$

The resulting model of the aircraft dynamics is of the form

$$\dot{x}_1 = x_2 \tag{9}$$

$$\dot{x}_2 = f(x) + G(x)u + \xi(x) \tag{10}$$

$$\dot{u} = -\lambda(u - u_c) \tag{11}$$

where $f(x) = f_1(x_1, F^{-1}(x_1)x_2)$, $G(x) = G_1(x_1, F^{-1}(x_1)x_2)$, and $\xi(x) = \xi_1[x_1, F^{-1}(x_1)x_2]$. The preceding model is now in a convenient form, and the design of a reference model is straightforward, as shown next. Because the state of the original system (z_1, z_2) is measurable, the state of the transformed system is also measurable because $x_1 = z_1$ and $x_2 = F(z_1)z_2$.

The desired dynamics of the aircraft in the transformed state space is now chosen in the form

$$\dot{x}_{m1} = x_{m2} \tag{12}$$

$$\dot{x}_{m2} = A_m x_m + B_m r \tag{13}$$

where $x_m = [x_{m1}^T \ \ x_{m2}]^T$ denotes the state of the reference model; $x_m : \mathbb{R}^+ \to \mathbb{R}^m$, matrix $A_0 = [[0 \ \ I]^T \ \ A_m^T]^T$ is asymptotically stable; and $r : \mathbb{R}^+ \to \mathbb{R}^p$ denotes a vector of bounded piecewise continuous reference inputs.

Control objective 1: In the case with no failures, design a control input $u_c(t)$ such that $\|x(t) - x_m(t)\| \le \epsilon$ for all time despite the effect of the disturbance $\xi(x(t))$.

III. Disturbance Rejection Controller

A baseline controller is first designed for the case when actuator dynamics can be neglected (i.e., $u = u_c$) and with no disturbances (i.e., $\xi \equiv 0$):

$$u_c = WG^T(x)[G(x)WG^T(x)]^{-1}[-f(x) + A_m x + B_m r] \tag{14}$$

where $W = W^T > 0$ denotes a control allocation matrix. Upon substituting expression (14) into Eq. (2), one obtains

$$\dot{x}_1 = x_2, \qquad \dot{x}_2 = A_m x + B_m r$$

The reference model equations (12) and (13) are subtracted from the preceding system next to obtain

$$\dot{e}_1 = e_2, \qquad \dot{e}_2 = A_m e$$

Because the matrix $A_0 = [[0 \ \ I]^T \ \ A_m^T]^T$ is asymptotically stable, it follows that $\lim_{t\to\infty} e(t) = 0$; hence, the control objective is achieved in the case with no disturbances and actuator dynamics.

In the case with disturbances, an observer is first designed in the form

$$\dot{\hat{x}}_1 = \hat{x}_2 \tag{15}$$

$$\dot{\hat{x}}_2 = A_m(\hat{x} - x) + f(x) + G(x)u + \hat{\xi} \tag{16}$$

where $\hat{\xi}$ denotes an estimate of ξ.

Because ξ is state dependent, standard adaptive control techniques cannot be used to estimate it. Hence, the focus is on the variable-structure-control approach.[13]

Variable Structure Observer: Let $\hat{e} = \hat{x} - x$ and $\hat{e}_i = \hat{x}_i - x_i$, $i = 1, 2$ denote the estimation errors. Upon subtracting the plant equation from expressions (15) and (16), one obtains

$$\dot{\hat{e}}_1 = \hat{e}_2 \tag{17}$$

$$\dot{e}_2 = A_m\hat{e} + \hat{\xi} - \xi \tag{18}$$

The preceding expression can be rewritten in a compact form as

$$\dot{\hat{e}} = A_0\hat{e} + C_0(\hat{\xi} - \xi) \tag{19}$$

where A_0 is defined earlier, and

$$C_0 = \begin{bmatrix} 0 \\ I_{p\times p} \end{bmatrix}$$

Let a tentative Lyapunov function be of the form

$$V(\hat{e}) = \tfrac{1}{2}\hat{e}^T P\hat{e}$$

where $P = P^T > 0$ is a solution to the Lyapunov matrix equation $A_0^T P + PA_0 = -Q$, where $Q = Q^T > 0$.

The first derivative of V along the motions of Eq. (19) yields

$$\dot{V}(\hat{e}) = -\tfrac{1}{2}\hat{e}^T Q\hat{e} + \hat{e}^T\bar{P}(\hat{\xi} - \xi)$$

where $\bar{P} = PC_0$. Let $\bar{P} = [p_{ij}]$. The preceding expression can be rewritten as

$$\dot{V}(\hat{e}) = -\frac{1}{2}\hat{e}^T Q\hat{e} + \sum_{i=1}^{p}(\hat{\xi}_i - \xi_i)\sum_{j=1}^{n} p_{ji}\hat{e}_j \le -\frac{1}{2}\hat{e}^T Q\hat{e} + \sum_{i=1}^{p}[c_i + d_i\varphi_i(x)]\sum_{j=1}^{n} p_{ji}\hat{e}_j + \sum_{i=1}^{p}\hat{\xi}_i\sum_{j=1}^{n} p_{ji}\hat{e}_j$$

The elements of the vector $\hat{\xi}$ are now chosen as

$$\hat{\xi}_i = -[c_i + d_i\varphi_i(x)]\ \text{sign}\left(\sum_{j=1}^{n} p_{ji}\hat{e}_j\right), \qquad i = 1, 2, \ldots, p \tag{20}$$

The derivative of V is now

$$\dot{V}(\hat{e}) \le -\frac{1}{2}\hat{e}^T Q\hat{e} + \sum_{i=1}^{p}[c_i + d_i\varphi_i(x)]\sum_{j=1}^{n} p_{ji}\hat{e}_j - \sum_{i=1}^{p}[c_i + d_i\varphi_i(x)]\left|\sum_{j=1}^{n} p_{ji}\hat{e}_j\right| \le -\frac{1}{2}\hat{e}^T Q\hat{e} < 0$$

hence $\hat{e}$ is bounded and $\lim_{t\to\infty}\hat{e}(t) = 0$.

The controller (14) is next modified as

$$u_c = WG^T(x)[G(x)WG^T(x)]^{-1}[-f(x) + A_m x + B_m r - \hat{\xi}] \quad (21)$$

Upon substituting the control input (21) into Eq. (16), one obtains

$$\dot{\hat{x}}_1 = \hat{x}_2, \qquad \dot{x}_2 = A_m \hat{x} + B_m r$$

The reference model (12) and (13) is next subtracted from the preceding expressions to obtain

$$\dot{e}_{m1} = e_{m2}, \qquad \dot{e}_{m2} = A_m e_m$$

where $e_m = \hat{x} - x_m$ and $e_{\mathrm{mi}} = \hat{x}_i - x_{\mathrm{mi}}$, $i = 1, 2$. Hence $\lim_{t\to\infty} e_m(t) = 0$. It is noted that $e_m = \hat{e} + e$, where $e = x - x_m$, denotes the tracking error, which implies that $e = e_m - \hat{e}$. Because $\hat{e}(t)$ has already been shown to tend to zero asymptotically, it follows that $\lim_{t\to\infty} e(t) = 0$, which ensures that the control objective is met.

Remark: The variable structure adaptive algorithm is robust to arbitrary time variations in the vector ξ. Its main disadvantage is that, because it contains a sign function, because of imperfections of the switching devices, it results in chattering of the signals in the system. Hence such algorithms are commonly approximated either by a saturation function or in the following way:

$$\operatorname{sign}(\eta) \cong \eta/(|\eta| + \delta)$$

where $0 < \delta \ll 1$. If the sign function in the algorithm (20) is approximated in such a way, the resulting tracking error will be ultimately uniformly bounded (UUB) rather than tend to zero asymptotically, and the size of the UUB set will depend on δ.

IV. Actuator Failures and Control Effector Damage

One of the important steps in the design of a FDIR system is failure and damage modeling and parameterization. In this section different failure and damage cases are described, and the corresponding mathematical models are given. The control objective under failures and damage is also stated.

A. Actuator Failures

Typical actuator failures include 1) lock in place (LIP); 2) hard-over failure (HOF); 3) float; and 4) loss of effectiveness (LOE). In the case of LIP failures, the actuator "freezes" at a certain condition and does not respond to subsequent commands. HOF is characterized by the actuator moving to and remaining at the upper or lower position limit regardless of the command. The speed of response is limited by the actuator rate limit. Float failure occurs when the actuator contributes zero moment to the control authority. Loss of effectiveness is characterized by lowering the actuator gain with respect to its nominal value. Different types of actuator failures are shown in Fig. 2.

Different types of actuator failures can be parameterized as follows:

$$u_i(t) = \begin{cases} u_{\mathrm{ci}}(t), & k_i(t) = 1, \quad \text{for all} \quad t \geq 0, \quad \text{no-failure case} \\ k_i(t)u_{\mathrm{ci}}(t), & 0 < \epsilon_i \leq k_i(t) < 1, \quad \text{for all} \quad t \geq t_{\mathrm{Fi}}, \quad \text{loss of effectiveness} \\ 0, & k_i(t) = 1, \quad \text{for all} \quad t \geq t_{\mathrm{Fi}}, \quad \text{float type of failure} \\ u_{\mathrm{ci}}(t_{\mathrm{Fi}}), & k_i(t) = 1, \quad \text{for all} \quad t \geq t_{\mathrm{Fi}}, \quad \text{lock-in-place failure} \\ (u_i)_{\min} \quad \text{or} \quad (u_i)_{\max}, & k_i(t) = 1, \quad \text{for all} \quad t \geq t_{\mathrm{Fi}}, \quad \text{hard-over failure} \end{cases}$$

where t_{Fi} denotes the time instant of failure of the ith actuator, k_i denotes its effectiveness coefficient such that $k_i \in [\epsilon_{\mathrm{ki}}, 1]$, and $\epsilon_{\mathrm{ki}} > 0$ denotes its minimum effectiveness.

In the case of first-order actuator dynamics, the class of failures just described can be modeled as follows:

$$\dot{u}_i = -\sigma_i \lambda_i (u_i - k_i u_{\mathrm{ci}}) \quad (22)$$

where $\lambda_i > 0$; $\sigma_i(t) = 1$ in the case of no failure, and $\sigma_i(t) = 0$, $u(t_{\mathrm{Fi}}) = \bar{u}_i$ when the failure occurs at $t = t_{\mathrm{Fi}}$, where t_{Fi} denotes the time of failure of the ith actuator. Hence in the case of failure at t_{Fi},

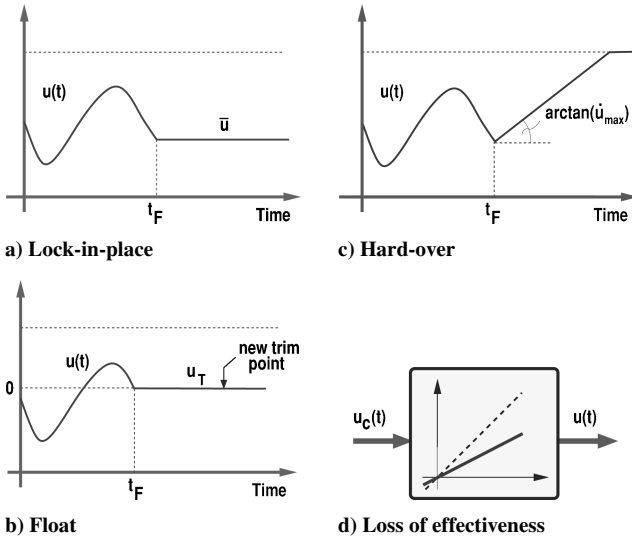

Fig. 2 Types of control effector failures.

one has that $\dot{u}_i(t) = 0$ for $t \geq t_{\mathrm{Fi}}$, and $u(t) = u(t_{\mathrm{Fi}})$ for all $t \geq t_{\mathrm{Fi}}$. In the case of LIP, $u(t_{\mathrm{Fi}})$ has the value of $u(t_{\mathrm{Fi}}^-)$, whereas in the case of HOF it moves to the upper or lower position limit.

B. Uncertainty

Uncertainty associated with each of the actuator models is caused by 1) unknown time of failure t_{Fi}, 2) unknown LOE coefficient k_i, and 3) unknown value at which the actuator locks.

C. Control Effector Damage

Control effector damage can be modeled using the diagonal control effector damage matrix D whose elements d_i are equal to one in the no-failure case (i.e., $D_N = I$), while in the case of control effector damage assume values over an interval $[\epsilon_{\mathrm{di}}, 1]$, where $\epsilon_{\mathrm{di}} \ll 1$, and each value of d is proportional to the percentage of the loss of surface. The resulting model is of the form

$$\dot{x}_1 = x_2 \quad (23)$$

$$\dot{x}_2 = f(x) + G(x)Du + \xi(x) \quad (24)$$

where $D = \operatorname{diag}[d_1 \;\; d_2 \ldots d_m]$, and $\xi(x)$ is a nonlinearity arising as a result of the asymmetry of the damaged aircraft such that, in the no-damage case, $\xi(x) = 0$.

The objective of this paper is to design a controller that will accommodate actuator failures and control effector damage even while compensating for the effect of the disturbance. Hence the following control objective will be considered:

Control objective 2: Design a control input $u_c(t)$ such that $\|x(t) - x_m(t)\| \leq \epsilon$ for all time despite the effect of the disturbance $\xi(x(t))$, actuator failures, and control effector damage.

V. Simultaneous Failure and Damage Accommodation and Disturbance Rejection

To design a reconfigurable controller that effectively compensates for the effect of LIP, LOE, HOF, or float failures, the expression (22) is first rewritten as

$$\dot{u}_i = -\lambda_i(u_i - \sigma_i k_i u_{\mathrm{ci}}) + \lambda_i(1 - \sigma_i)u_i \quad (25)$$

The preceding expression is next divided by λ_i, and singular perturbation arguments are used to obtain

$$u_i \cong \sigma_i k_i u_{\mathrm{ci}} + (1-\sigma_i)\bar{u}_i,$$

where $\bar{u}_i = u_i(t_{\mathrm{Fi}})$, that is, $\bar{u}_i$ is the value at which the actuator has locked at the time of failure. The preceding equation is next substituted into Eq. (2) to obtain

$$\dot{x}_1 = x_2 \tag{26}$$

$$\dot{x}_2 = f(x) + \sum_{i=1}^{m} g_i(x) d_i [\sigma_i k_i u_{\mathrm{ci}} + (1-\sigma_i)\bar{u}_i] + \xi(x) \tag{27}$$

It is seen that the presence of $\bar{u}_i$ in the preceding expression introduces additional uncertainty into the model. For this reason the following assertion is considered.

Assertion 1: If $\sigma \in \{0, 1\}$, then $(1-\sigma_i)(\bar{u}_i - u_i) \equiv 0$.

Proof: The proof follows trivially because the assertion is true for $\sigma_i = 1$, whereas for $\sigma_i = 0$, which happens at t_{Fi}, one has that $u_i(t_{\mathrm{Fi}}) = \bar{u}_i$. ∎

Based on the result of the preceding assertion, the model (27) is now rewritten as

$$\dot{x}_1 = x_2 \tag{28}$$

$$\dot{x}_2 = f(x) + \sum_{i=1}^{m} g_i(x) d_i [\sigma_i k_i u_{\mathrm{ci}} + (1-\sigma_i) u_i] + \xi(x) \tag{29}$$

Expression (29) describes the plant under a class of potential failures and damage described in the preceding section and will be used in the FDIR design as described next.

A. Decentralized Adaptive FDI Observer

The decentralized FDI observer for estimating actuator failure-related parameters is first built in the form

$$\dot{\hat{u}}_i = -\hat{\sigma}_i \lambda (u_i - \hat{k}_i u_{\mathrm{ci}}) - \lambda_0 (\hat{u}_i - u_i) \tag{30}$$

where $\lambda_0 > 0$.

Let $\hat{e}_{\mathrm{ui}} = \hat{u}_i - u_i$. Upon subtracting Eq. (22) from Eq. (30), one obtains

$$\begin{aligned}\dot{\hat{e}}_{\mathrm{ui}} &= -\lambda_0 \hat{e}_{\mathrm{ui}} - \lambda \phi_{\sigma i} u_i + \lambda(\hat{\sigma}_i \hat{k}_i u_{\mathrm{ci}} - \sigma_i k_i u_{\mathrm{ci}}) \\ &= -\lambda_0 \hat{e}_{\mathrm{ui}} + \lambda \sigma_i \phi_{\mathrm{ki}} u_{\mathrm{ci}} - \lambda(u_i - \hat{k}_i u_{\mathrm{ci}})\phi_{\sigma i} \\ &= -\lambda_0 \hat{e}_{\mathrm{ui}} + \phi_i^T \omega_i \end{aligned} \tag{31}$$

where $\phi_{\sigma i} = \hat{\sigma}_i - \sigma_i$, $\phi_{\mathrm{ki}} = \hat{k}_i - k_i$, $\phi_i = [\phi_{\sigma_i} \;\; \phi_{\mathrm{ki}}]^T$, and $\omega_i = \lambda[-(u_i - \hat{k}_i u_{\mathrm{ci}}) \;\; \sigma_i u_{\mathrm{ci}}]^T$.

B. Global Robust FDI Observer

The next step is to design an observer, based on expressions (28) and (29), for estimation of the effect of damage and state-dependent disturbances:

$$\dot{\hat{x}}_1 = \hat{x}_2 \tag{32}$$

$$\dot{\hat{x}}_2 = A_m(\hat{x} - x) + f(x) + \left\{ \sum_{i=1}^{m} g_i(x) \hat{d}_i [\hat{\sigma}_i \hat{k}_i u_{\mathrm{ci}} + (1-\hat{\sigma}_i) u_i] \right\} + \hat{\xi} \tag{33}$$

where the estimates $\hat{\sigma}_i$ and $\hat{k}_i$ are generated by the decentralized FDI subsystem.

Let $\phi_{\mathrm{di}} = \hat{d}_i - d_i$, $\hat{e} = \hat{x} - x$, and

$$\hat{D} = \mathrm{diag}[\hat{d}_1 \quad \hat{d}_2 \ldots \hat{d}_m] \tag{34}$$

$$\hat{K} = \mathrm{diag}[\hat{k}_1 \quad \hat{k}_2 \ldots \hat{m}_m] \tag{35}$$

$$\hat{\Sigma} = \mathrm{diag}[\hat{\sigma}_1 \quad \hat{\sigma}_2 \ldots \hat{\sigma}_m] \tag{36}$$

$$\tilde{G}_0(x) = [g_1(x)\hat{\sigma}_1 \quad g_2(x)\hat{\sigma}_2 \ldots g_m(x)\hat{\sigma}_m] \tag{37}$$

and let $U = \mathrm{diag}[u]$ and $\hat{d} = \mathrm{diag}[\hat{D}]$. To ensure the invertibility of $\tilde{G}_0$, at least p of the estimates σ_i are kept at value one for all time (compare assumption 1e).

Now the following theorem is considered.

Theorem 1: The following control law for the system (28) and (29):

$$u_c = \hat{D}\hat{K}\tilde{G}_0^T \left(\tilde{G}_0 \hat{D}^2 \hat{K}^2 \tilde{G}_0^T\right)^{-1} [-f(x) + A_m x + B_m r - G(x)(I - \hat{\Sigma})u - \hat{\xi}]$$

where the estimates are adjusted by using

$$\dot{\hat{\sigma}}_i = \dot{\phi}_{\sigma i} = \mathrm{Proj}_{[0,1]}\{\gamma_{\sigma i}(u_i - \hat{k}_i u_{\mathrm{ci}})\hat{e}_i\}, \qquad i = 1, 2, \ldots, m \tag{38}$$

$$\dot{\hat{k}}_i = \dot{\phi}_{\mathrm{ki}} = \mathrm{Proj}_{[\epsilon_{\mathrm{ki}}, 1]}\{-\gamma_{\mathrm{ki}} u_{\mathrm{ci}} \hat{e}_i\}, \qquad i = 1, 2, \ldots, m \tag{39}$$

$$\dot{\hat{d}}_i = \mathrm{Proj}_{[\epsilon_{\mathrm{di}}, 1]}\{1 - \mathrm{sign}[u_i \hat{e}^T \bar{P} g_i(x)]\} \tag{40}$$

$$\dot{\hat{\xi}}_i = -\left[c_i + d_i \varphi_i(x) + \sum_{i=1}^{m} |g_i(x)\omega_i| \right] \mathrm{sign}\left(\sum_{j=1}^{n} p_{\mathrm{ji}} \hat{e}_j \right) \qquad i = 1, 2, \ldots, p \tag{41}$$

where $\gamma_{\sigma i} > 0$, $\gamma_{\mathrm{ki}} > 0$, and $\gamma_{\mathrm{di}} > 0$, ensures the boundedness of all signals in the system and, in addition, $\lim_{t\to\infty}[x(t) - x_m(t)] = 0$, and $\lim_{t\to\infty} \hat{e}_{\mathrm{ui}}(t) = 0$, $i = 1, 2, \ldots, m$. (In the preceding equations Proj$\{\cdot\}$denotes the projection operator[14] the role of which is to project the estimates $\hat{\sigma}_i$, $\hat{k}_i$, and $\hat{d}_i$ to the intervals $[0, 1]$, $[\epsilon_{\mathrm{ki}}, 1]$, and $[\epsilon_{\mathrm{di}}, 1]$, respectively.)

Before proceeding to the proof of the theorem, the following assertion is considered.

Assertion 2: Let $d \in [\epsilon_d, 1]$ and

$$\hat{d} = \mathrm{Proj}_{[\epsilon_d, 1]}\{1 - \mathrm{sign}(\omega)\} \tag{42}$$

Then $\omega(\hat{d} - d) \le 0$, for all $\hat{d} \in [\epsilon_d, 1]$, all $d \in [\epsilon_d, 1]$, and all ω.

Proof: The proof is based on considering two cases. The first case is when $1 - \mathrm{sign}(\omega) < 1$, which implies that $\hat{d} = 1 - \mathrm{sign}(\omega)$. In such a case one has that

$$\hat{d}\omega = \omega - |\omega|, \qquad \omega\hat{d} - \omega d = \omega(1-d) - |\omega| \le 0$$

In the second case one has that $1 - \mathrm{sign}(\omega) \ge 1$, which also implies that $\hat{d} = 1$. From this inequality it also follows that $\mathrm{sign}(\omega) \le 0$ and $\omega \le 0$; hence,

$$-|\omega| + |\omega| d \le 0$$

because $d \le 1$, which completes the proof. ∎

Proof of Theorem 1: The proof is divided into two parts. In the first part the objective is to demonstrate that the decentralized estimation of actuator failure-related parameters yields bounded estimation errors, whereas in the second part it will be shown that the preceding algorithms ensure effective compensation for the effect of state-dependent disturbances, control effector damage, and the coupling between the decentralized estimation subsystem and the damage and disturbance estimation subsystem.

The following tentative Lyapunov function is chosen first:

$$V(\hat{e}_{\mathrm{ui}}, \phi_{\sigma i}, \phi_{\mathrm{ki}}) = \tfrac{1}{2}\left\{ \hat{e}_{\mathrm{ui}}^2 + \lambda[\phi_{\sigma i}/\gamma_{\sigma i} + \sigma_i(\phi_{\mathrm{ki}}/\gamma_{\mathrm{ki}})] \right\}$$

Hence, V is positive semidefinite if $\sigma_i = 0$. Its first derivative along the motions of the system yields

$$\dot{V}(\hat{e}_{\mathrm{ui}}, \phi_{\sigma i}, \phi_{\mathrm{ki}}) \le -\lambda_0 \hat{e}_{\mathrm{ui}}^2 \le 0$$

The latter inequality holds regardless of the value of σ_i. Because adaptive algorithms with projection are used, $\hat{k}_i$ will always be

bounded, along with $\hat{\sigma}_i$. From the derivative of V, one can conclude that $\hat{e}_{\text{ui}}$ is bounded. It can also be readily demonstrated that $\hat{e}_{\text{ui}} \in \mathcal{L}^2$. However, it cannot yet be concluded that this error tends to zero asymptotically.

The global FDI observer (32) and (33) is now written as

$$\dot{\hat{x}}_1 = \hat{x}_2 \tag{43}$$

$$\dot{\hat{x}}_2 = A_m(\hat{x} - x) + f(x) + G(x)\hat{D}[\hat{\Sigma}\hat{K}u_c + (I - \hat{\Sigma}_i)u] + \hat{\xi} \tag{44}$$

Because $\hat{D}$, $\hat{K}$, and $\hat{\Sigma}$ are diagonal, one has that $G(x)\hat{D}\hat{\Sigma}\hat{K} = G(x)\hat{\Sigma}\hat{D}\hat{K} = G_0(x)\hat{D}\hat{K}$.

Substituting the control law (38) into the preceding observer equation results in the following closed-loop observer system:

$$\dot{\hat{x}}_1 = \hat{x}_2, \qquad \dot{\hat{x}}_2 = A_m\hat{x} + B_m r$$

Upon subtracting the reference model equations, it can be readily shown that the error between the observer and the reference model will tend to zero. Because the state of the reference model x_m is bounded, it follows that $\hat{x}$ is bounded as well. However, it remains to be shown that x is also bounded.

Recalling that $\hat{e} = \hat{x} - x$ and $\hat{e}_i = \hat{x}_i - x_i$, $i = 1, 2$, subtracting the expressions (28) and (29) from Eqs. (32) and (33) yields

$$\dot{\hat{e}}_1 = \hat{e}_2 \tag{45}$$

$$\dot{\hat{e}}_2 = A_m e + G(x)U(\hat{d} - d) + \hat{\xi} - \xi + \sum_{i=1}^{m} g_i(x)\hat{d}_i\phi_i^T\omega_i \tag{46}$$

where $d = \text{diag}[D]$ and $\hat{d}$ and U were defined earlier.

The expressions (45) and (46) can be rewritten in a compact form as

$$\dot{\hat{e}} = A_0\hat{e} + C_0\left[GU(\hat{d} - d) + \hat{\xi} - \xi + \sum_{i=1}^{m} g_i(x)\phi_i\omega_i\right] \tag{47}$$

where A_0 and C_0 were defined earlier.

Let a tentative Lyapunov function be of the form

$$V(\hat{e}) = \tfrac{1}{2}\hat{e}^T P\hat{e}$$

where $P = P^T > 0$ is a solution to the Lyapunov matrix equation $A_0^T P + PA_0 = -Q$, where $Q = Q^T > 0$.

The first derivative of V along the motions of Eq. (47) yields

$$\dot{V}(\hat{e}) = -\frac{1}{2}\hat{e}^T Q\hat{e} + \hat{e}^T\bar{P}G(x)U(\hat{d} - d) + \hat{e}^T\bar{P}\left[\hat{\xi} - \xi + \sum_{i=1}^{m} g_i(x)\phi_i\omega_i\right]$$

where $\bar{P} = PC_0$. Using the assertion 2 and the adjustment law for $\hat{d}$ given by Eq. (40), the derivative of V becomes

$$\dot{V}(\hat{e}) \le -\frac{1}{2}\hat{e}^T Q\hat{e} + \hat{e}^T\bar{P}\left[\hat{\xi} - \xi + \sum_{i=1}^{m} g_i(x)\phi_i\omega_i\right]$$

The preceding expression can be rewritten as

$$\dot{V}(\hat{e}) = -\frac{1}{2}\hat{e}^T Q\hat{e} + \sum_{i=1}^{p}\left[\xi_i - \hat{\xi}_i + \sum_{i=1}^{m} g_i(x)\phi_i\omega_i\right]\sum_{j=1}^{n} p_{\text{ji}}\hat{e}_j$$

$$\le -\frac{1}{2}\hat{e}^T Q\hat{e} + \sum_{i=1}^{p}\left[c_i + d_i\varphi_i(x) + \sum_{i=1}^{m}|g_i(x)\omega_i|\right]\sum_{j=1}^{n} p_{\text{ji}}\hat{e}_j + \sum_{i=1}^{p}\hat{\xi}_i\sum_{j=1}^{n} p_{\text{ji}}\hat{e}_j$$

Using expression (41), the derivative of V is now

$$\dot{V}(\hat{e}) \le -\frac{1}{2}\hat{e}^T Q\hat{e} + \sum_{i=1}^{p}\left[c_i + d_i\varphi_i(x) + \sum_{i=1}^{m}|g_i(x)\omega_i|\right]\sum_{j=1}^{n} p_{\text{ji}}\hat{e}_j$$

$$- \sum_{i=1}^{p}\left[c_i + d_i\varphi_i(x) + \sum_{i=1}^{m}|g_i(x)\omega_i|\right]\left|\sum_{j=1}^{n} p_{\text{ji}}\hat{e}_j\right|$$

$$\le -\frac{1}{2}\hat{e}^T Q\hat{e} < 0$$

hence, $\hat{e}$ is bounded, and $\lim_{t\to\infty}\hat{e}(t) = 0$.

Because it has been already shown that $\lim_{t\to\infty}[\hat{x}(t) - x_m(t)] = 0$ and because $e_m = \hat{e} + e$, where $e = x - x_m$ denotes the tracking error, it follows that x is bounded and that $\lim_{t\to\infty} e(t) = 0$. It can now be readily verified that $\hat{e}_{\text{ui}}$ is bounded, which, using the fact that $\hat{e}_{\text{ui}} \in \mathcal{L}^\infty \cap \mathcal{L}^2$, implies that $\lim_{t\to\infty}\hat{e}_{\text{ui}}(t) = 0$, $i = 1, 2, \ldots, m$. ■

One can again use the approximation

$$\text{sign}(\eta) \cong \eta/(|\eta| + \delta)$$

where $0 < \delta \ll 1$, to prevent chattering and ensure the UUB of the signals in the system.

VI. Simulations

In this section the results of performance evaluation of the robust integrated FDIR scheme on a simulation of the Boeing's TAFA are presented. The results presented are for the case of lateral doublet. Recent performance evaluations of a simplified version of the proposed integrated FDIR system through F/A-18 piloted simulations are also briefly described.

A. TAFA Simulations

The TAFA is a conceptual design of an advanced fighter configuration that blends an extensive suite of conventional and innovative control effectors to achieve high agility in a low observable design. The TAFA is a single-engine, single-seat fighter designed for air-to-air and/or air-to-ground missions. In this paper the focus is on the flight condition with altitude at the sea level, Mach number 0.9, and an angle of attack of 1.65 deg.

A linearized model of TAFA dynamics is of the form

$$\Delta\dot{x} = A\Delta x + B\Delta u \tag{48}$$

The states of the linearized TAFA dynamics are $\Delta x = [\Delta V\ \Delta q\ \Delta\theta\ \Delta\alpha\ \Delta h\ \Delta\beta\ \Delta p\ \Delta r\ \Delta\phi\ \Delta\psi]^T$, where ΔV denotes perturbed forward velocity, Δq denotes the perturbed pitch rate, $\Delta\theta$ denotes the perturbed pitch angle, $\Delta\alpha$ denotes the perturbed angle of attack, Δh denotes the perturbed altitude, $\Delta\beta$ denote the perturbed sideslip angle, Δp and Δr denote respectively the perturbed roll and yaw rates, and $\Delta\phi$ and $\Delta\psi$ denote respectively the perturbed bank and yaw angles, where all perturbations are with respect to a trim. The control inputs of TAFA are given as follows: Δu_1, perturbed left trailing-edge flap deflection (TEFL), rad; Δu_2, perturbed left canard deflection (CNDL), rad; Δu_3, perturbed pitch thrust vectoring nozzle deflection (NOZp), rad; Δu_4, perturbed left aft-body flap deflection (ABFL), rad; Δu_5, perturbed left aileron deflection (AILL), rad; Δu_6, perturbed right aileron deflection (AILR), rad; Δu_7, perturbed right aft-body flap deflection (ABFR), rad; Δu_8, perturbed right trailing-edge flap deflection (TEFR), rad; Δu_9, perturbed right canard deflection (CNDR), rad; Δu_{10}, perturbed yaw thrust-vectoring nozzle deflection (NOZy), rad; Δu_{11}, perturbed differential leading-edge flap deflection (DfLEF), rad; and Δu_{12}, perturbed continuous moldline deflection (DCMUP), rad.

The linearized stability and control derivative matrices for TAFA dynamics around this flight condition are of the form

$$A = \begin{bmatrix} -0.06 & -27.25 & -32.21 & 75.93 & 0 & 0 & 0 & 0 & 0 & 0 \\ 0 & -4.28 & 0 & 8.74 & 0 & 0 & 0 & 0 & 0 & 0 \\ 0 & 1 & 0 & 0 & 0 & 0 & 0 & 0 & 0 & 0 \\ 0 & 1 & 0 & -1.86 & 0 & 0 & 0 & 0 & 0 & 0 \\ 0 & 0 & 1004.8 & -1004.8 & 0 & 0 & 0 & 0 & 0 & 0 \\ 0 & 0 & 0 & 0 & 0 & -0.12 & 0.03 & -1 & 0.03 & 0 \\ 0 & 0 & 0 & 0 & 0 & -30.85 & -5.81 & 0.03 & 0 & 0 \\ 0 & 0 & 0 & 0 & 0 & -11.67 & 0.04 & -0.55 & 0 & 0 \\ 0 & 0 & 0 & 0 & 0 & 0 & 1 & 0.03 & 0 & 0 \\ 0 & 0 & 0 & 0 & 0 & 0 & 0 & 1 & 0 & 0 \end{bmatrix}$$

$$B = \begin{bmatrix} -0.31 & 20.38 & 0 & -5.18 & 0.12 & 0.12 & -5.18 & -0.31 & 20.38 & 0 & 0 & 0 \\ -14.07 & 14.93 & -3.94 & 0 & -6.23 & -6.23 & 0 & -14.07 & 14.93 & 0 & 0 & 0 \\ 0 & 0 & 0 & 0 & 0 & 0 & 0 & 0 & 0 & 0 & 0 & 0 \\ -0.15 & -0.03 & -0.02 & 0 & -0.06 & -0.06 & 0 & -0.15 & -0.03 & 0 & 0 & 0 \\ 0 & 0 & 0 & 0 & 0 & 0 & 0 & 0 & 0 & 0 & 0 & 0 \\ -0.02 & 0.01 & 0 & 0.02 & 0 & 0 & -0.02 & 0.02 & -0.01 & 0.02 & -0.01 & 0 \\ 49.9 & 3.88 & 0 & 0.15 & 34.72 & -34.72 & -0.15 & -49.9 & -3.88 & 0.12 & 104.73 & -1034.6 \\ 2.45 & 3.6 & 0 & -4.24 & 0.46 & -0.46 & 4.24 & -2.45 & -3.6 & -3.44 & 4.74 & 2.9 \cdot 10^4 \\ 0 & 0 & 0 & 0 & 0 & 0 & 0 & 0 & 0 & 0 & 0 & 0 \\ 0 & 0 & 0 & 0 & 0 & 0 & 0 & 0 & 0 & 0 & 0 & 0 \end{bmatrix}$$

Table 1 Position and rate limits on the control effectors

Effector	Position limit, deg	Rate limit, deg/s
Left trailing-edge flap	[−30, 45]	[−90, 90]
Left canard	[−80, 10]	[−70, 70]
NOZp - pitch thrust-vectoring nozzle	[−30, 30]	[−70,70]
Left aftbody flap	[0, 90]	[−120, 120]
Left aileron	[−30, 30]	[−120, 120]
Right aileron	[−30, 30]	[−120, 120]
Right aftbody flap	[0, 90]	[−120, 120]
Right trailing-edge flap	[−30, 45]	[−90,90]
Right canard	[−80, 10]	[−70, 70]
NOZy-yaw thrust-vectoring nozzle	[−30, 30]	[−60, 60]
Differential leading-edge flaps	[−30, 30]	[−70, 70]

1. Actuator Dynamics, Position, and Rate Limits

All actuators are characterized by first-order dynamics of the form

$$u = [40/(s + 40)]u_c$$

where u is the actual position of the effector and u_c is the position command for that effector generated by the controller.

The input vector $u = [u_1 \ldots u_{12}]$ defined earlier is expressed in terms deflections of the left and right flaps. Their position and rate limits are listed in Table 1.

2. Medium-Fidelity Nonlinear Simulation of TAFA Dynamics

The simulation takes into account the rotation from the attitude angles to the body angular rates, Coriolis acceleration, and the effects of gravity, whereas aerodynamic forces and moments are approximated by the terms from the stability and control derivative matrices. All position and rate limits and actuator dynamics are included in the simulation, along with actuator failures (LIP, LOE) and control effector damage.

3. FDIR System Design and Implementation

The nonlinear model used for simulation of TAFA dynamics was transformed along the lines described in Sec. II, and, when the actuator failures and control effector damage are included, has the form (23) and (24). The transformed system states are θ, ϕ, ψ, q, p, r, V, α, and β. The controller is given by Eq. (38), and parameter adjustment laws are given by Eqs. (38–41).

4. Simulation Scenario

The simulation scenario consists of a lateral doublet (maximum magnitude $\phi = 60$ deg). No command in ψ is specified, which makes this a demanding maneuver for the TAFA. At time $t = 3.5$ s, the aircraft undergoes multiple simultaneous failures and damage. The complete failure scenario consists of 1) two lock-in-place failures of the left canard (CNDL) and left aftbody flap (ABFL); 2) surface damage to the left trailing-edge flap (TEFL) and left aileron (AILL) such that $d_{\text{TEFL}} = 0.2$ and $d_{\text{AILL}} = 0.2$; and 3) a disturbance input caused by the damage. The damage-generated disturbance is assumed to cause nonlinear effects in the angular rates p, q, and r, of the form

$$\xi_q = -4\alpha^2 - 10\beta^2 + -2p^2 - 4q^2 - 8r^2 - 2pq - 2pr - 4qr \tag{49}$$

$$\xi_p = -10\alpha^2 - 6\beta^2 - 2p^2 - 6q^2 - 16r^2 - 4pq - 4pr - 2qr \tag{50}$$

$$\xi_r = -2\alpha^2 - 10\beta^2 - 6p^2 - 10q^2 - 4r^2 - 8pq - 8pr - 2qr \tag{51}$$

It is seen that the damage is assumed to result in a large nonlinearity. This type of disturbance was chosen because the p, q, r squared and cross terms represent the type of effect that arises when damage causes asymmetry in the vehicle kinematics. The α and β terms were included to model aerodynamic effects caused by the damage. In the simulations, because the main maneuver is in p, the p^2 term generally dominates.

5. Controller Parameters

The bounds on the nonlinearity are assumed to be of the form

$$\varphi_p = \varphi_q = \varphi_r = 20(|\alpha| + |\beta| + |p| + |q| + |r|)^2 \tag{52}$$

which will always be larger in magnitude than the true disturbance, while having a similar form. The adaptive gains were chosen as $\gamma_{\sigma i} = 500$ and $\gamma_{\text{ki}} = 5$. The adaptive observer gain is $\lambda = 40$.

6. Reference Model

The reference model matrices are given next. It is noted that, for the desired dynamics of V, α, and β, the elements of the A_m and B_m matrices are chosen from the corresponding diagonal elements of the A matrix:

$$A_m = \begin{bmatrix} A_{11} & 0 & 0 & 0 & 0 & 0 & 0 & 0 & 0 & 0 \\ 0 & -7 & -25 & 0 & 0 & 0 & 0 & 0 & 0 & 0 \\ 0 & 1 & 0 & 0 & 0 & 0 & 0 & 0 & 0 & 0 \\ 0 & 1 & 0 & A_{44} & 0 & 0 & 0 & 0 & 0 & 0 \\ 0 & 0 & A_{53} & A_{54} & 0 & 0 & 0 & 0 & 0 & 0 \\ 0 & 0 & 0 & 0 & 0 & A_{66} & 0 & -1 & 0 & 0 \\ 0 & 0 & 0 & 0 & 0 & 0 & -7 & 0 & -25 & 0 \\ 0 & 0 & 0 & 0 & 0 & 0 & 0 & -7 & 0 & -25 \\ 0 & 0 & 0 & 0 & 0 & 0 & 1 & 0 & 0 & 0 \\ 0 & 0 & 0 & 0 & 0 & 0 & 0 & 1 & 0 & 0 \end{bmatrix}$$

$$B_m = \begin{bmatrix} -A_{11} & 0 & 0 & 0 & 0 & 0 \\ 0 & 0 & 25 & 0 & 0 & 0 \\ 0 & 0 & 0 & 0 & 0 & 0 \\ 0 & -A_{44} & 0 & 0 & 0 & 0 \\ 0 & 0 & 0 & 0 & 0 & 0 \\ 0 & 0 & 0 & -A_{66} & 0 & 0 \\ 0 & 0 & 0 & 0 & 25 & 0 \\ 0 & 0 & 0 & 0 & 0 & 25 \\ 0 & 0 & 0 & 0 & 0 & 0 \\ 0 & 0 & 0 & 0 & 0 & 0 \end{bmatrix}$$

7. Simulations

All simulations are run with the proposed integrated FDIR system. The following cases are included: 1) nominal (no-failure/no-damage) case; 2) actuator lock-in-place only (no damage/no disturbances); 3) control effector damage with a resulting disturbance (no actuator failures); and 4) the full-failure scenario, in which there are simultaneous actuator failures and control effector damage with resulting disturbance, as just described. The baseline controller that has no reconfiguration capability provides poor performance in case 2, and is not capable of stabilizing the system in cases 3 and 4. The simulations with the proposed integrated FDIR system are detailed next.

Nominal case. First a nominal simulation is presented where there are no failures or damage. The proposed integrated FDIR system is running throughout the simulation and does not generate any false alarms. (The performance is identical to that of an unreconfigurable baseline controller.) The resulting response is shown in Figs. 3–5.

Actuator lock-in-place failures only. In this case the aircraft suffers lock-in-place failures of the left canard (CNDL) and left aftbody flap (ABFL) at $t = 3.5$ s. The resulting response is shown in Fig. 6–9. It is seen that the system is stabilized, and the resulting response is comparable to that obtained in the no-failure case.

Control effector damage and disturbance only. In this case the left trailing-edge flap (TEFL) and left aileron (AILL) undergo damage at $t = 3.5$ s, and their remaining effectiveness is 0.2, that is, $d_{\text{TEFL}} = 0.2$ and $d_{\text{AILL}} = 0.2$. The damage-generated disturbance is of the form (49–51). The response of the system is shown in Figs. 10–12. It is seen that, after a transient, the system stabilizes at trim, and that the tracking in ϕ is accurate.

Simultaneous actuator lock in place and control effector damage. This is the most challenging scenario, in which the two preceding failure scenarios are combined. In this case, the aircraft suffers two lock-in-place actuator failures, two cases of control effector damage, and a large resulting disturbance. The response of the system is shown in Figs. 13–16. It is seen that the response is good and that the actuator lock in place is accurately identified.

B. F/A-18 Simulations

An integral part of the proposed robust integrated FDIR system is the decentralized FDIR algorithms, also referred to as the FLARE (Fast on-Line Actuator Recovery Enhancement) system, developed under a NASA Dryden Small Business Innovation Research (SBIR) project[15] for the case of flight-critical actuator failures. The FLARE algorithms were recently evaluated at Boeing through high-fidelity and piloted simulations of the F/A-18C/D aircraft under lock-in-place and hard-over actuator failures.[16] Because the FLARE system was developed for a linearized model of F/A-18

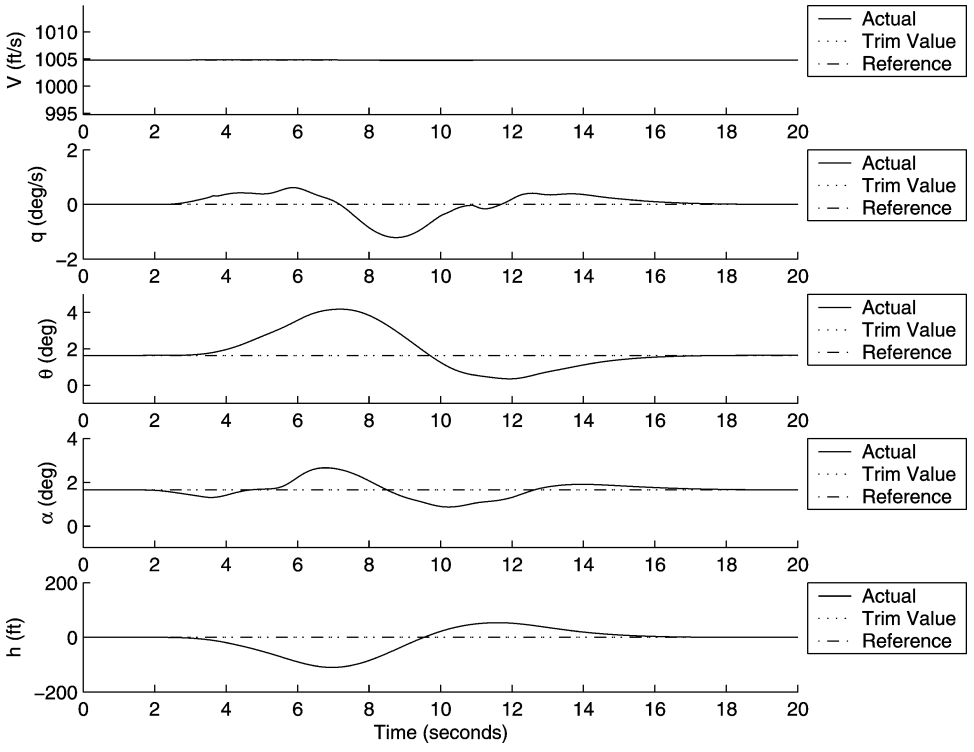

Fig. 3 Longitudinal state response with the proposed FDIR system in the no-failure/no-damage case.

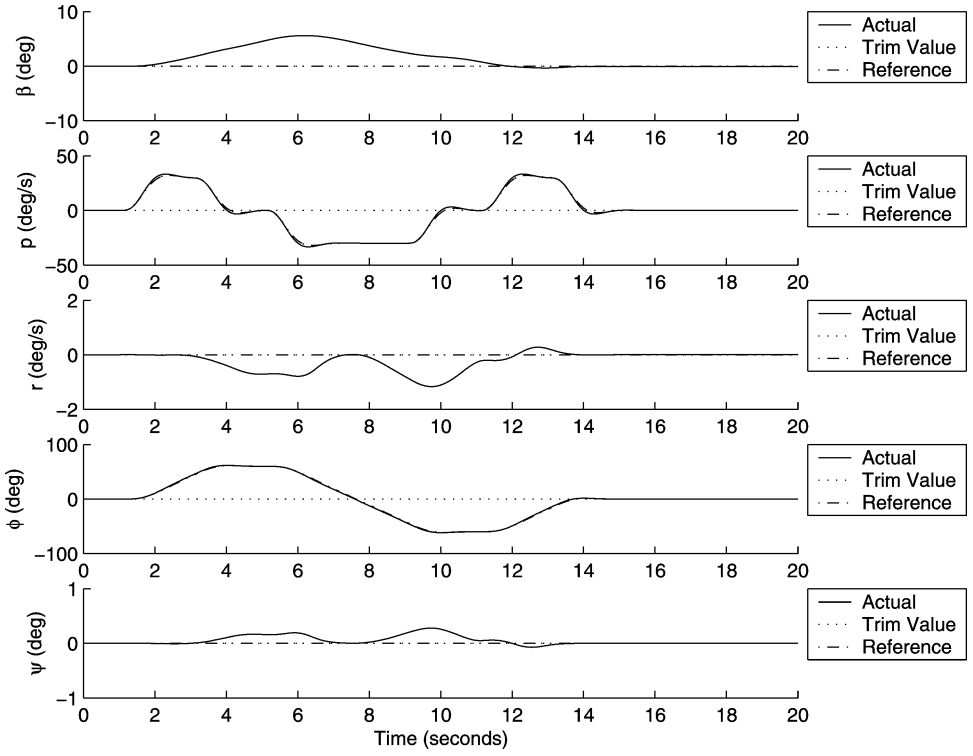

Fig. 4 Lateral state response with the proposed FDIR system in the no-failure/no-damage case.

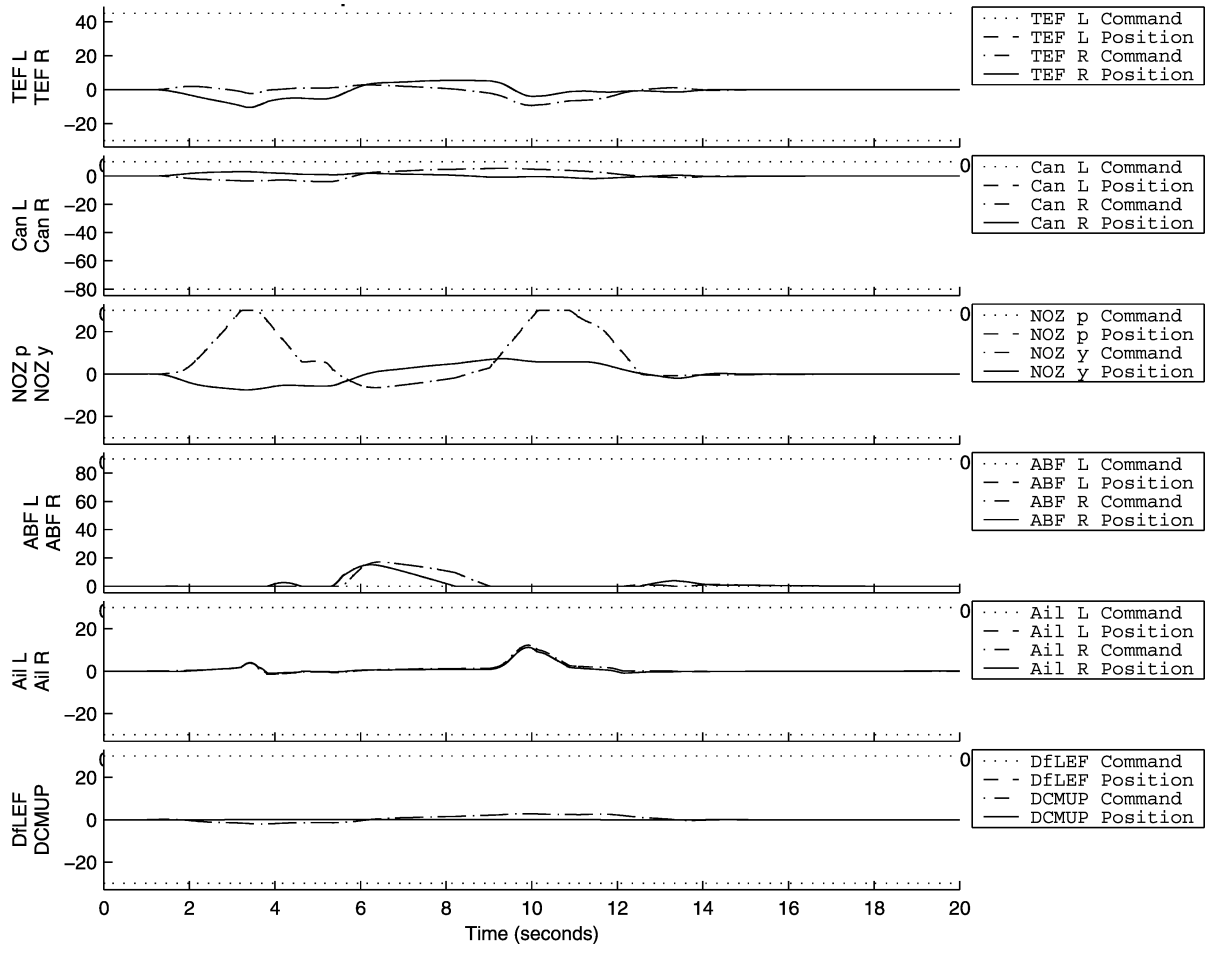

Fig. 5 Control input response with the proposed FDIR system in the no-failure/no-damage case.

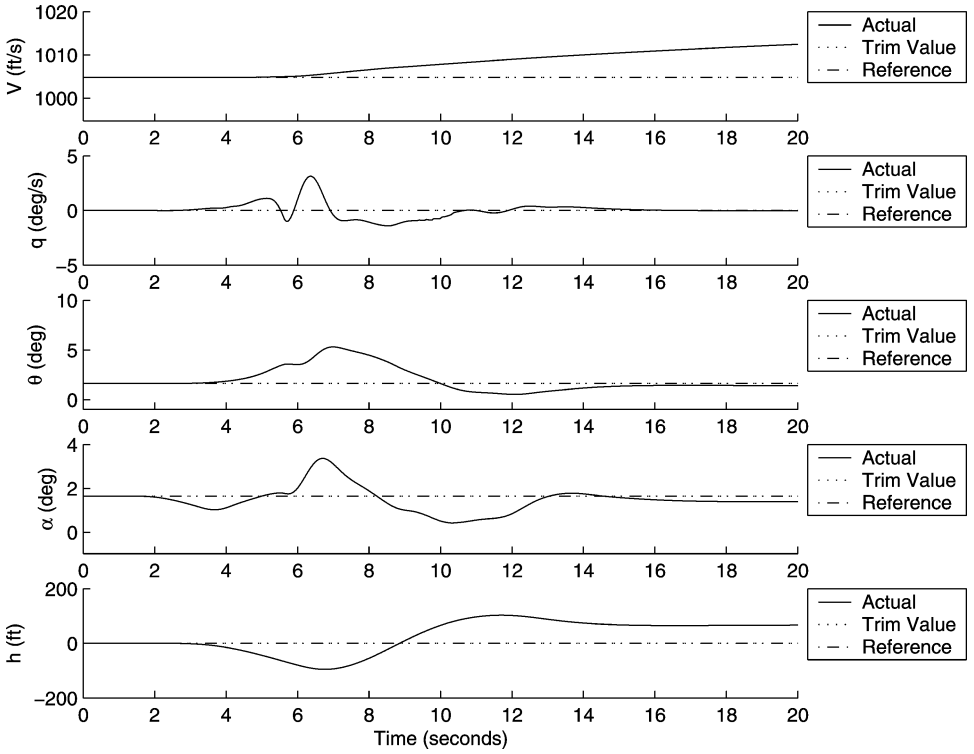

Fig. 6 Longitudinal state response with the proposed FDIR system in the case of actuator lock-in-place.

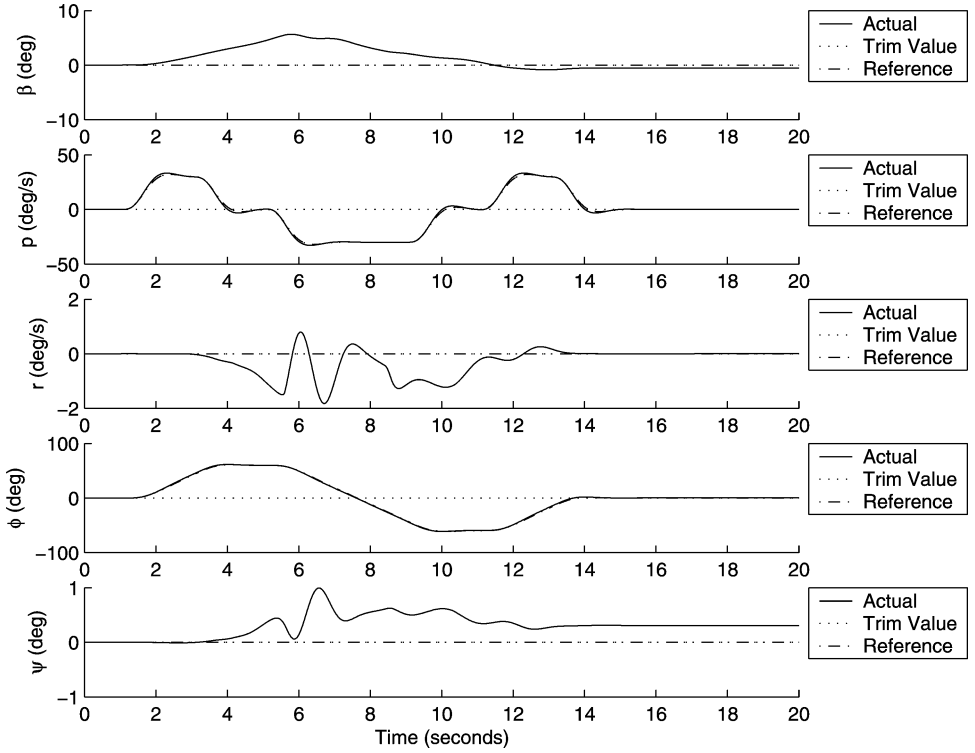

Fig. 7 Lateral state response with the proposed FDIR system in the case of actuator lock-in-place.

dynamics, the scheme also includes variable-structure compensation of unmodeled dynamics caused by linearization. The design was initially carried out in MATLAB® by using a low-fidelity F/A-18 simulation and was subsequently evaluated on a high-fidelity F/A-18 simulation at Boeing. Following successful evaluations on the high-fidelity simulator, the FLARE algorithms were imported into the piloted flight simulator at Boeing, and their performance was evaluated by a pilot during longitudinal and lateral doublets, a 4-*g* turn, a 360-deg roll, and tracking tasks using Cooper–Harper rating scale. The results of the piloted simulations in the case of aileron, rudder, and stabilator failures are summarized in Fig. 17. The aileron and rudder underwent lock-in-place failures at 0 and 15 deg and hard-over failures to their position limits of ±30 deg, while the stabilator was locked at 0, 3, and 6 deg. It is seen that the FLARE system substantially improves the flight performance under flight-critical failures, and, in some cases, the failure and its subsequent accommodation were barely noticeable by the pilot.

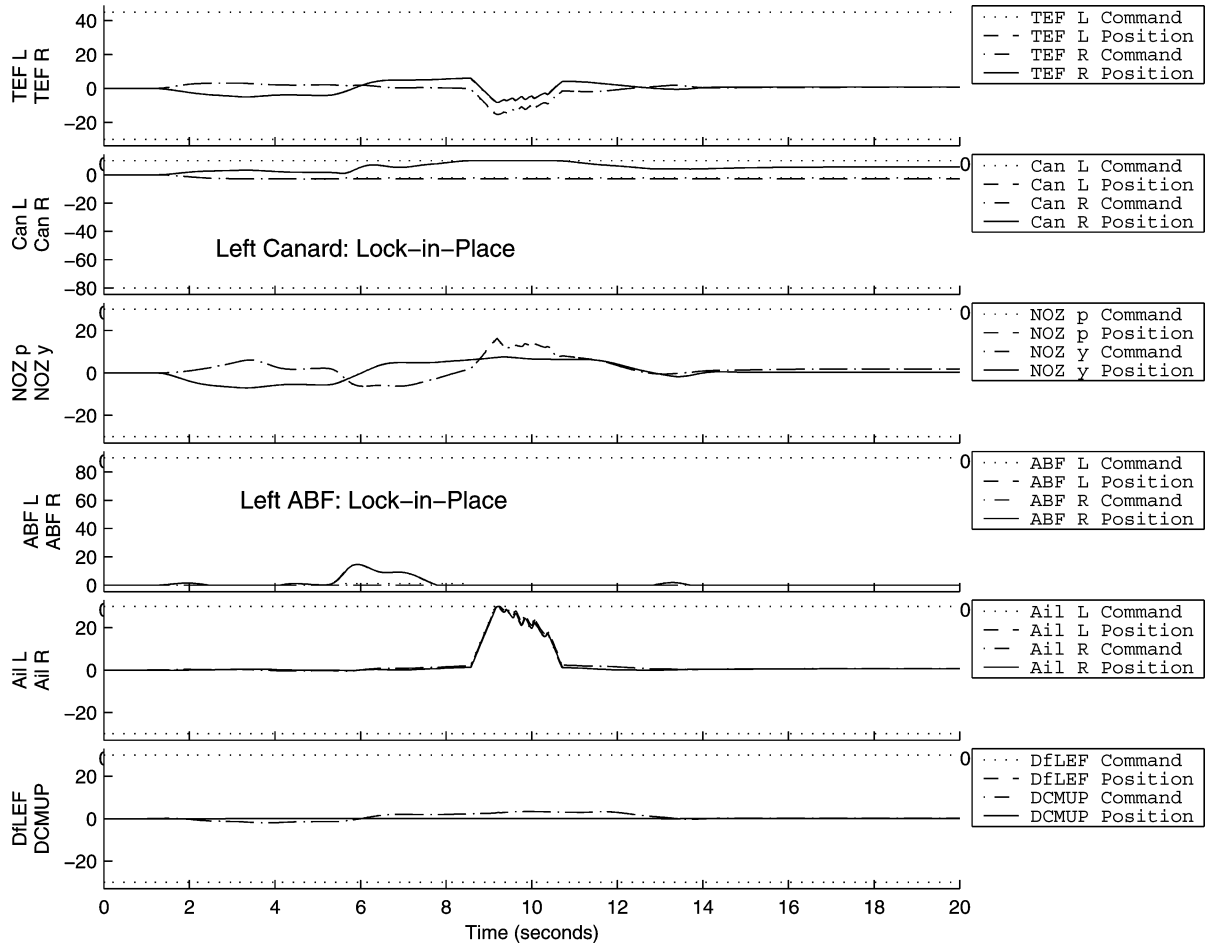

Fig. 8 Control input response with the proposed FDIR system in the case of actuator lock-in-place.

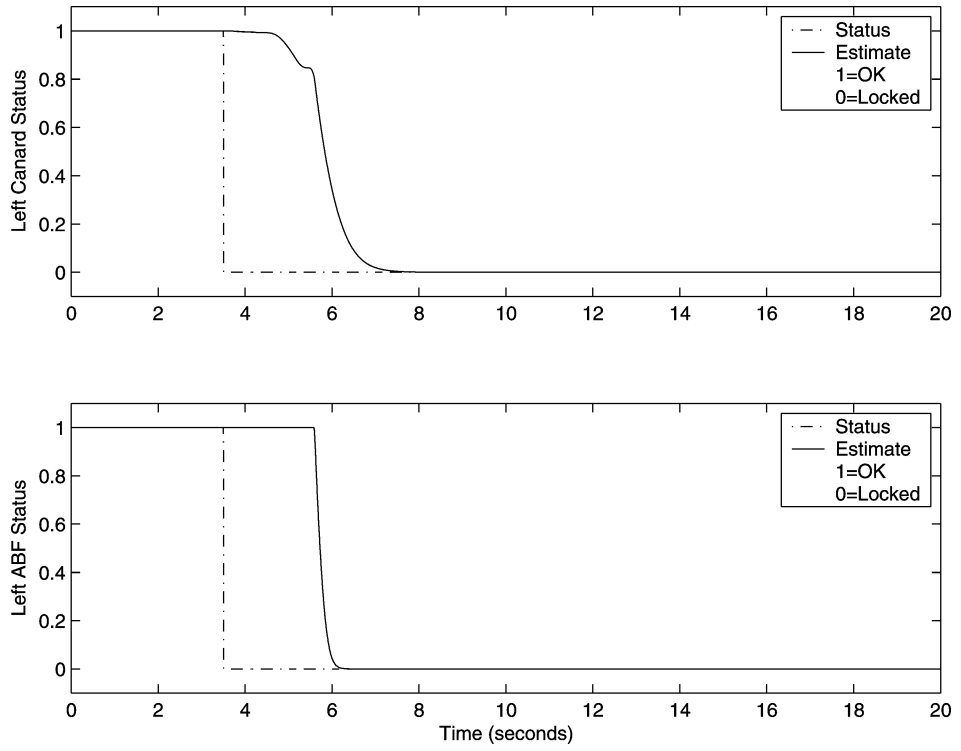

Fig. 9 Actuator failure parameter estimates in the case of actuator lock-in-place.

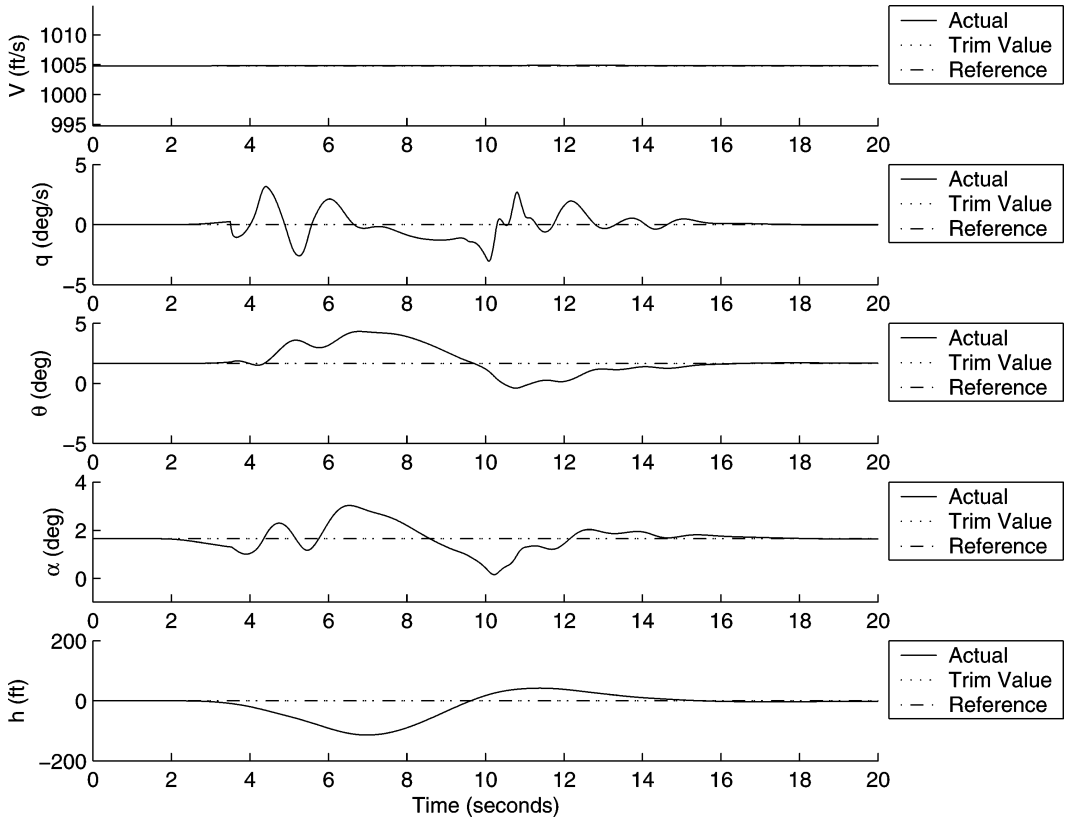

Fig. 10 Longitudinal state response with the proposed FDIR system in the case of control effector damage.

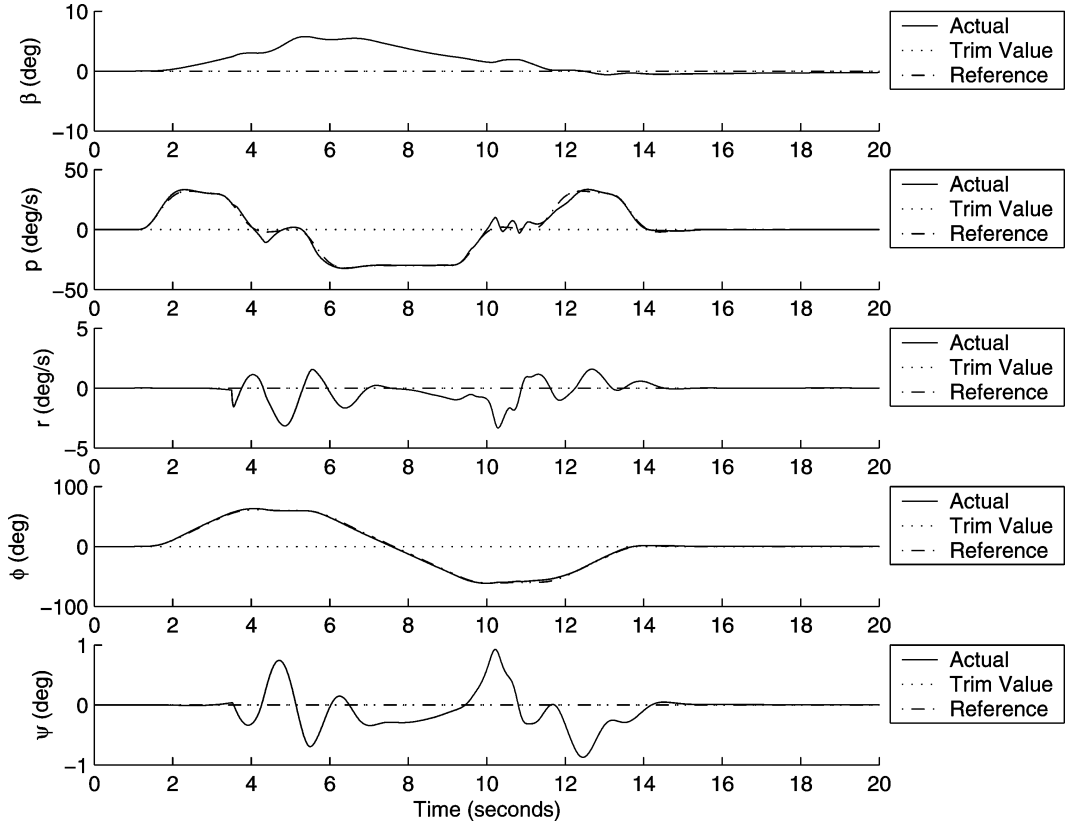

Fig. 11 Lateral state response with the proposed FDIR system in the case of control effector damage.

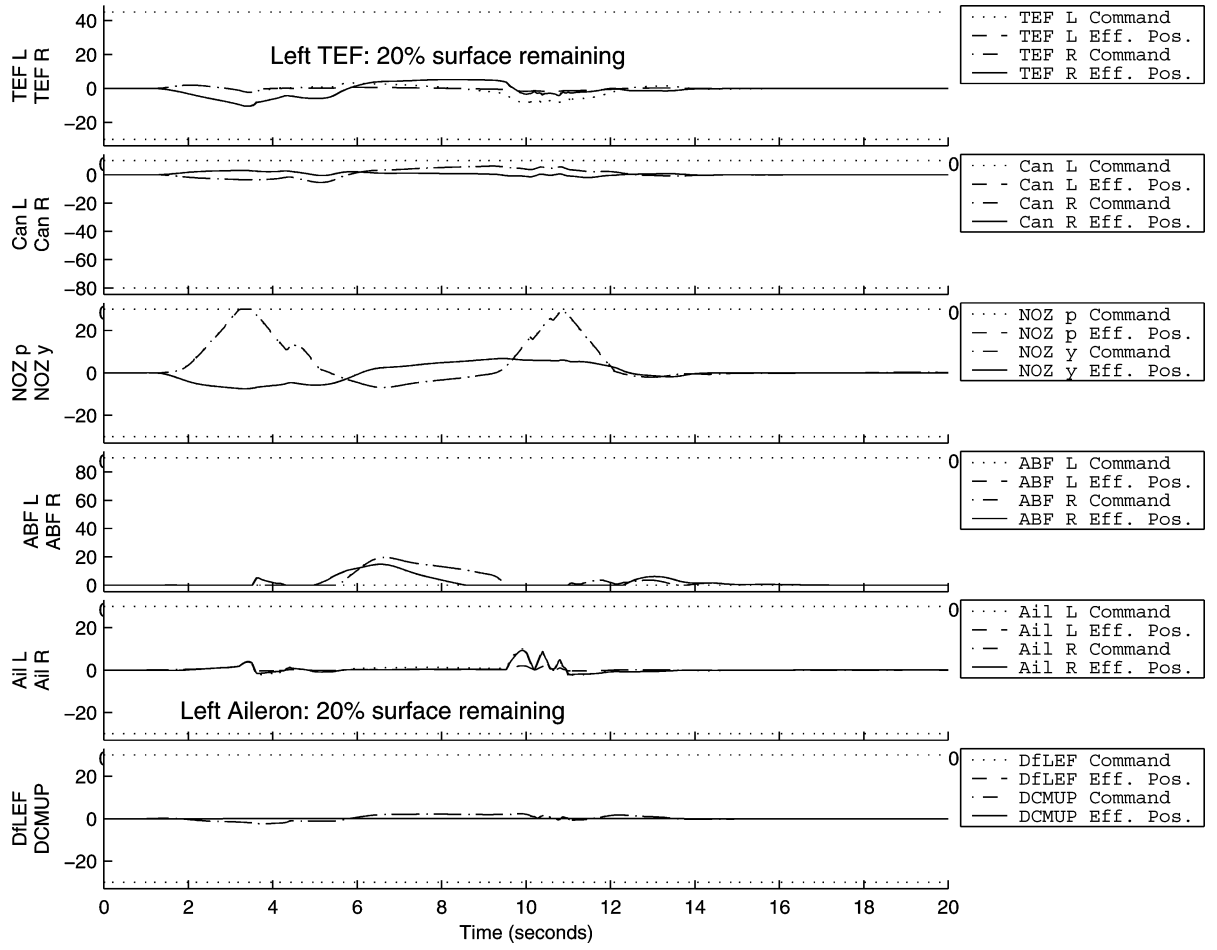

Fig. 12 Control input response with the proposed FDIR system in the case of control effector damage.

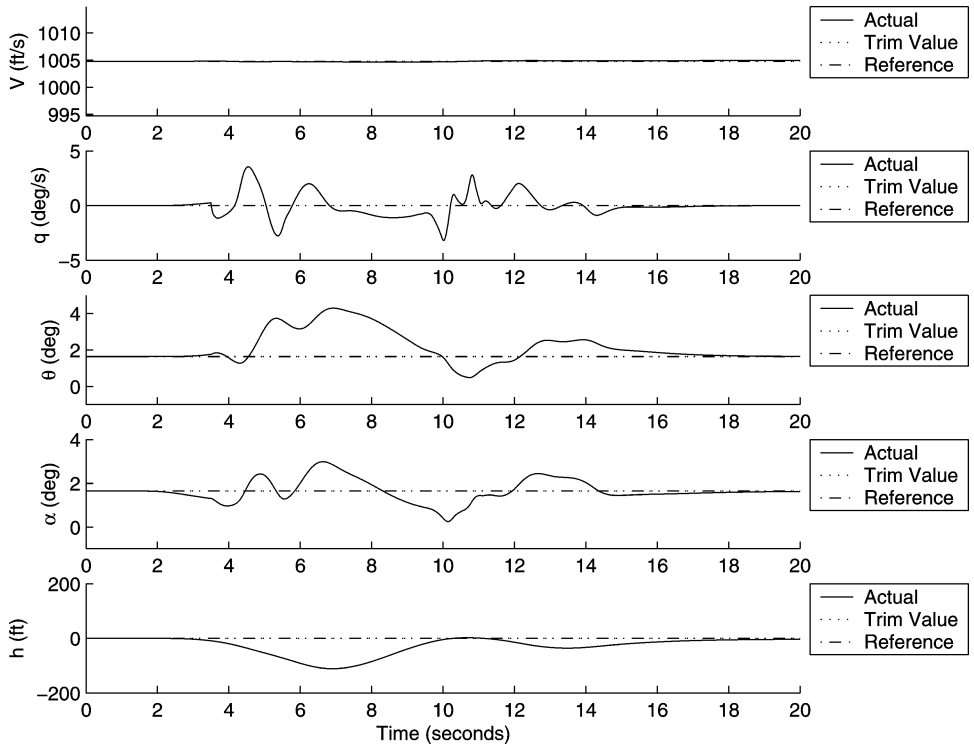

Fig. 13 Longitudinal state response with the proposed FDIR system in the case of simultaneous actuator failures and control effector damage.

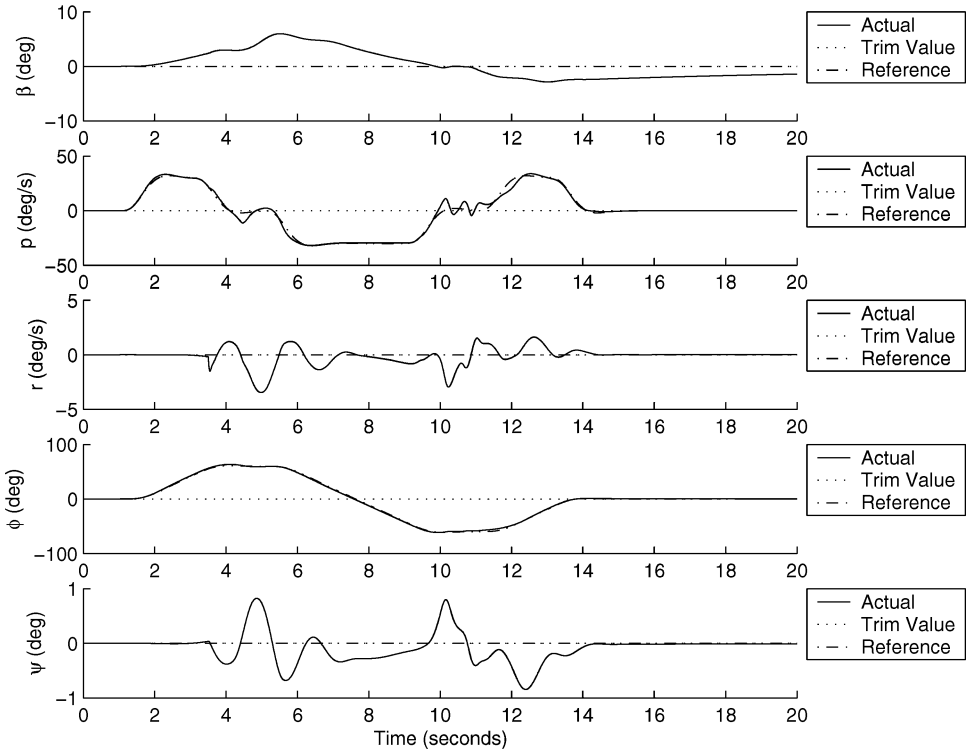

Fig. 14 Lateral state response with the proposed FDIR system in the case of simultaneous actuator failures and control effector damage.

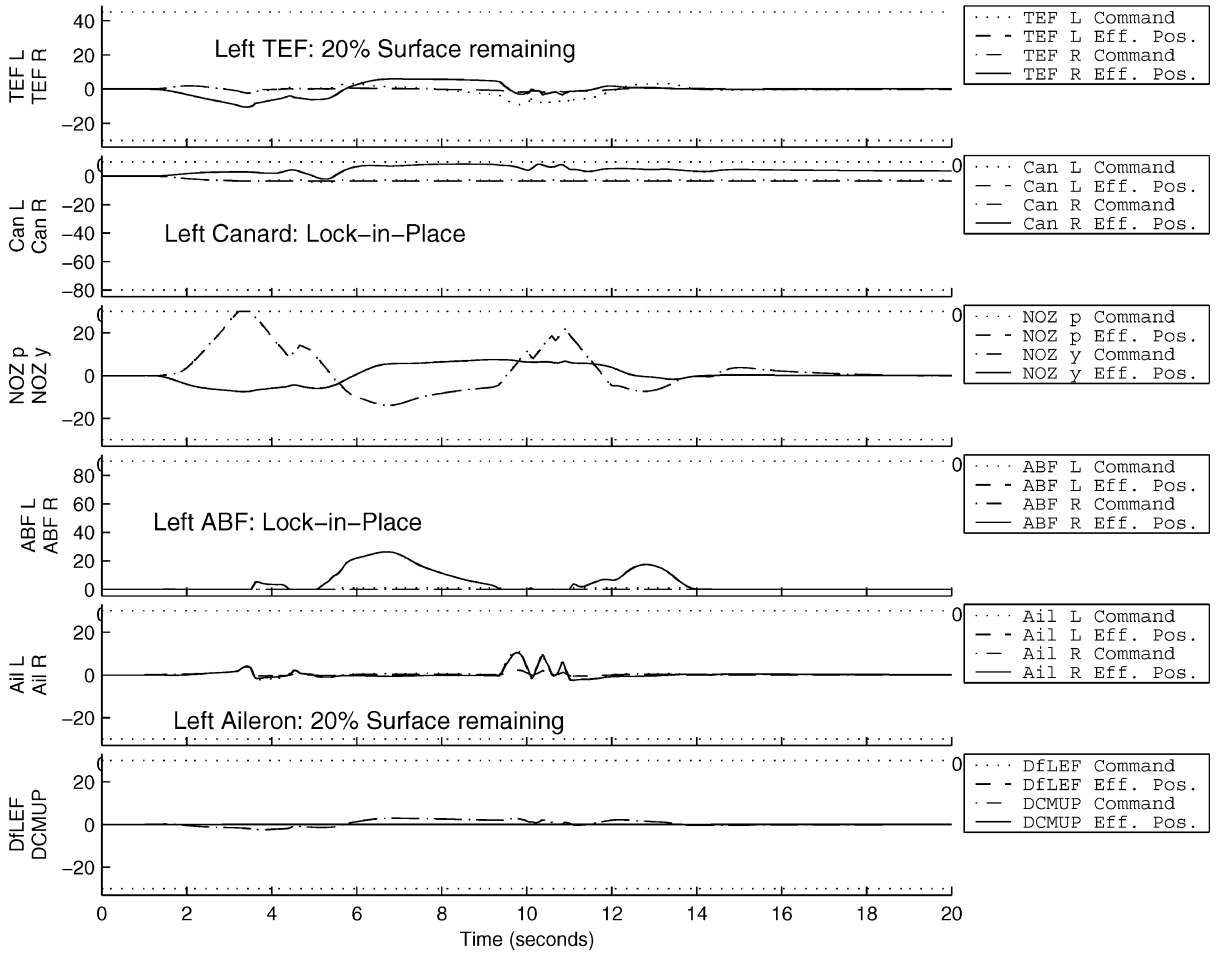

Fig. 15 Control input response with the proposed FDIR system in the case of simultaneous actuator failures and control effector damage.

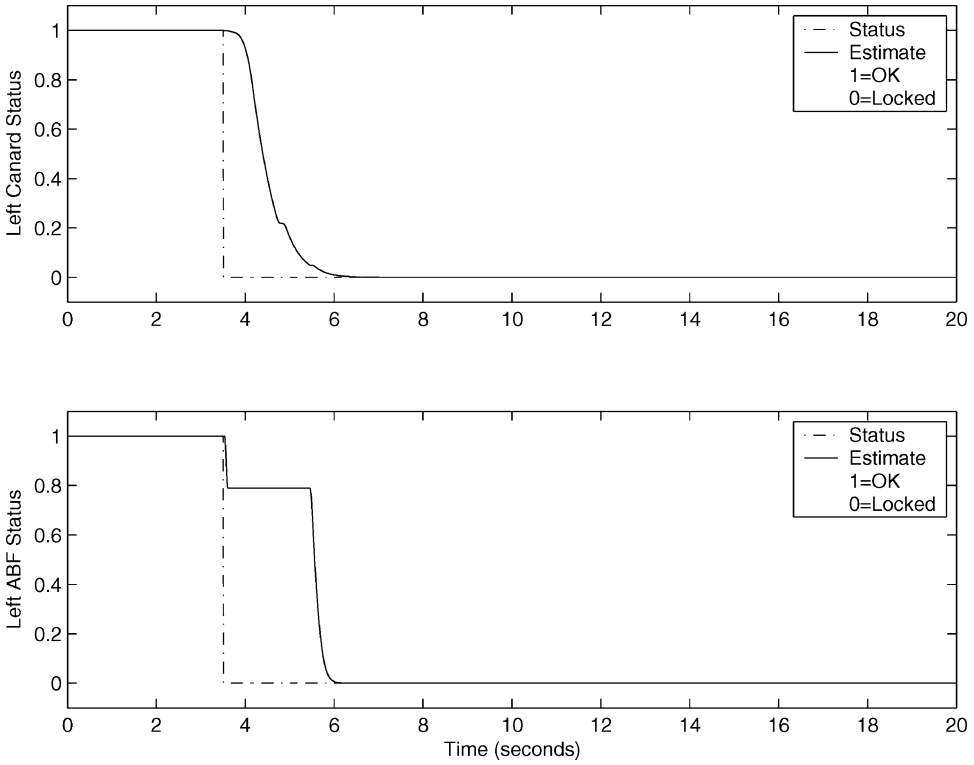

Fig. 16 Actuator failure parameter estimates with the proposed FDIR system in the case of simultaneous actuator failures and control effector damage.

		Stabilator Failures						Aileron Failures						Rudder Failures		
		Trim		3 deg.		6 deg.		15 degrees				30 deg.		Trim	15	30
		Dbl	Trk	Dbl	Trk	Dbl	Trk	Dbl	Trk	4G	Roll	Dbl	Trk	Dbl	Dbl	Trk
Flight Condition A: Mach 0.7, 20,000 ft.	Baseline Aircraft w/o Failures	2	3	2	3	2	3	2	3	2	2	2	3	2	2	2
	Baseline Aircraft with Failures	4	6	6	5.5	7	7+	5	7	6	5	8	7-8	2.5	3.5	3.5-4
	Failures with FLARE	2.5	4.5	4	4	3.5	3.5-4	3.5	3.5	3-4	3	4	4	2	2	2.25
Flight Condition B: Mach 0.6, 30,000 ft.	Baseline Aircraft w/o Failures	3				3	4	3	4	4		3	4		2	2.5
	Baseline Aircraft with Failures	4	N/A			5	7	5	5	6	N/A	6	6	N/A	3.5	4.5
	Failures with FLARE	3				3	4	3	4	4		4	4		2	2.75

Dbl = Doublet Task: Pilot performs stick maneuvers beginning with 1/4 stick, increasing to full stick.
Trk = Tracking Task: Pilot tracks another aircraft through a series of demanding maneuvers.
4G = 4G Turn: Pilot makes a sharp turn at or near 4G of force on the pilot. Failure occurs during the turn.
Roll = 360 Roll: Pilot rolls the aircraft through 360 degrees, and returns it to level flight. Failure occurs in the middle of the roll.

2 to 3 had very favorable pilot comments
3.5 to 4.5 had favorable pilot comments
5 to 6 had negative pilot comments
7 and higher had very negative pilot comments

Fig. 17 Results of Cooper–Harper evaluation of FLARE under aileron, rudder, and stabilator failures.

VII. Conclusions

In the paper, a robust integrated fault-tolerant flight control system that accommodates for different types of actuator failures and control effector damage is presented even while rejecting state-dependent disturbances. It is shown that variable structure laws for the adjustment of disturbance estimates yield a stable system despite simultaneous presence of failures, damage, and disturbances. The properties of the proposed algorithms are illustrated on a medium-fidelity simulation of Boeing's Tailless Advanced Fighter Aircraft. The implementation of the FLARE system, which represents an integral part of the proposed failure, detection, identification, and reconfiguration system, on a piloted simulator of F/A-18 aircraft is also described.

The results presented in the paper appear fairly promising considering that the proposed system achieves acceptable performance despite two locked actuators, two damaged control effectors, and a large disturbance affecting all three angular rates. Future plans include extensive testing of the proposed algorithms on a high-fidelity simulator and their implementation to other manned and unmanned vehicles.

Acknowledgment

This research was partially supported by the NASA Dryden Flight Research Center under Contract NAS4-02017 to Scientific Systems Company.

References

[1]Bodson, M., and Groszkiewicz, J., "Multivariable Adaptive Algorithms for Reconfigurable Flight Control," *IEEE Transactions on Control Systems Technology*, Vol. 5, No. 2, 1997, pp. 217–229.

[2]Ahmed-Zaid, F., Ioannou, P., Gousman, K., and Rooney, R., "Accommodation of Failures in the F-16 Aircraft Using Adaptive Control," *IEEE Control Systems Magazine*, Vol. 11, No. 1, 1991, pp. 73–78.

[3]Monaco, J. D., Ward, D., Barron, R., and Bird, R., "Implementation and Flight Test Assessment of an Adaptive, Reconfigurable Flight Control System," AIAA Paper 97-3738, Aug. 1997.

[4]Chandler, P., Pachter, M., and Mears, M., "System Identification for Adaptive and Reconfigurable Control," *Journal of Guidance, Control, and Dynamics*, Vol. 18, No. 3, 1995, pp. 516–524.

[5]Calise, A., Lee, S., and Sharma, M., "Direct Adaptive Reconfigurable Control of a Tailless Fighter Aircraft," *Proceedings of the 1998 AIAA*

Guidance, Navigation, and Control Conference, Vol. 1, Reston, VA, 1998, pp. 88–97.

[6]Brinker, J., and Wise, K., "Reconfigurable Flight Control of a Tailless Advanced Fighter Aircraft," *Proceedings of the 1998 AIAA Guidance, Navigation, and Control Conference*, Vol. 1, AIAA, Reston, VA, 1998, pp. 75–87.

[7]Brinker, J., and Wise, K., "Flight Testing of a Reconfigurable Flight Control Law on the X-36 Tailless Fighter Aircraft," AIAA Paper 2000-3941, Aug. 2000.

[8]Bošković, J. D., and Mehra, R. K., "A Decentralized Scheme for Autonomous Compensation of Multiple Simultaneous Flight-Critical Failures," AIAA Paper 2002-4453, Aug. 2002.

[9]Bošković, J. D., and Mehra, R. K., "An Adaptive Scheme for Compensation of Loss of Effectiveness of Flight Control Effectors," *Proceedings of the 40th IEEE Conference on Decision and Control*, Vol. 3, Inst. of Electrical and Electronics Engineers, Piscataway, NJ, 2001, pp. 2448–2453.

[10]Bošković, J. D., and Mehra, R. K., "Intelligent Adaptive Control of a Tailless Advanced Fighter Aircraft Under Wing Damage," *Journal of Guidance, Control, and Dynamics*, Vol. 23, No. 5, 2000, pp. 876–884.

[11]Wise, K., and Sedwick, J., "Stability Analysis of Reconfigurable and Gain Scheduled Flight Control System Using LMIs," *Proceedings of the 1998 AIAA Guidance, Navigation, and Control Conference*, Vol. 1, Reston, VA, 1998, pp. 118–126.

[12]Bošković, J. D., and Mehra, R. K., "Robust Fault-Tolerant Control Design for Aircraft Under State-Dependent Disturbances," AIAA Paper 2003-5490, Aug. 2003.

[13]Hsu, L., and Costa, R., "Variable Structure Model Reference Adaptive Control Using Only I/O Measurements," *International Journal of Control*, Vol. 49, No. 2, 1989, pp. 399–416.

[14]Bošković, J. D., and Mehra, R. K., "A Multiple Model Adaptive Flight Control Scheme for Accommodation of Actuator Failures," *Journal of Guidance, Control, and Dynamics*, Vol. 25, No. 4, 2002, pp. 712–724.

[15]Bošković, J. D., Bergstrom, S. E., and Mehra, R. K., "Aircraft Prognostics and Health Management (PHM) and Adaptive Reconfigurable Control (ARC) System," NASA DFRC Phase II SBIR, Final Rept., Contract NAS4-02017, March 2004.

[16]Bošković, J. D., Bergstrom, S. E., Mehra, R. K., Urnes, J. M., Sr., Hood, M., and Lin, Y., "Performance Evaluation of an Integrated Retrofit Failure Detection, Identification and Reconfiguration (FDIR) System Using High-Fidelity and Piloted Simulations," Society of Automotive Engineers, SAE Paper 2004-01-3115, Nov. 2004.